

Effects of Graphite/Partially Carbonized Hemp Hurd Particle Mass Ratios on
Tribological Properties of Polybenzoxazine Composites



A Thesis Submitted in Partial Fulfillment of the Requirements
for the Degree of Master of Engineering in Chemical Engineering

Department of Chemical Engineering

FACULTY OF ENGINEERING

Chulalongkorn University

Academic Year 2019

Copyright of Chulalongkorn University

ผลของอัตราส่วนโดยมวลของแกรไฟต์/ถ่านแกนกัญชง ต่อสมบัติทางโทรโปโลยีในวัสดุพอลิเบนซอก
ซาซีนคอมพอสิต



วิทยานิพนธ์นี้เป็นส่วนหนึ่งของการศึกษาตามหลักสูตรปริญญาวิศวกรรมศาสตรมหาบัณฑิต
สาขาวิชาวิศวกรรมเคมี ภาควิชาวิศวกรรมเคมี
คณะวิศวกรรมศาสตร์ จุฬาลงกรณ์มหาวิทยาลัย
ปีการศึกษา 2562
ลิขสิทธิ์ของจุฬาลงกรณ์มหาวิทยาลัย

Thesis Title	Effects of Graphite/Partially Carbonized Hemp Hurd Particle Mass Ratios on Tribological Properties of Polybenzoxazine Composites
By	Miss Nuttarika Kunaroop
Field of Study	Chemical Engineering
Thesis Advisor	Professor SARAWUT RIMDUSIT, Ph.D.
Thesis Co Advisor	Associate Professor Chanchira Jubslip, D.Eng.

Accepted by the FACULTY OF ENGINEERING, Chulalongkorn University in
Partial Fulfillment of the Requirement for the Master of Engineering

..... Dean of the FACULTY OF
ENGINEERING
(Professor SUPOT TEACHAVORASINSKUN, D.Eng.)

THESIS COMMITTEE

..... Chairman
(Assistant Professor AMORNCHAI ARPORNWICHANOP,
D.Eng.)

..... Thesis Advisor
(Professor SARAWUT RIMDUSIT, Ph.D.)

..... Thesis Co-Advisor
(Associate Professor Chanchira Jubslip, D.Eng.)

..... Examiner
(CHALIDA KLAYSOM, Ph.D.)

..... External Examiner
(Passarin Jongvisuttisun, Ph.D.)

ณัฐริกา คุณารูป : ผลของอัตราส่วนโดยมวลของแกรไฟต์/ถ่านแกนกัญชง ต่อสมบัติทาง
 ไทรโบโลยีในวัสดุพอลิเบนซอกซาซีนคอมพอสิต. (Effects of Graphite/Partially
 Carbonized Hemp Hurd Particle Mass Ratios on Tribological Properties of
 Polybenzoxazine Composites) อ.ที่ปรึกษาหลัก : ศ. ดร.ศราวุธ ริมดุสิต, อ.ที่ปรึกษา
 ร่วม : รศ. ดร.จันจิรา จัปศิลป์

งานวิจัยนี้มีวัตถุประสงค์เพื่อศึกษาผลของสารตัดแปรความเสียดทานสองชนิด คือ แกร
 ไฟท์สังเคราะห์และถ่านแกนกัญชง ทางด้านเสถียรภาพทางความร้อน สมบัติเชิงกลแบบไดนามิก
 สมบัติเชิงกล รวมไปถึงสมบัติด้านไทรโบโลยีของวัสดุเสียดทานชนิดพอลิเบนซอกซาซีนคอมพอสิต
 รวมทั้งทำการสร้างแบบจำลองผ้าเบรกและจานหมุน โดยใช้โปรแกรมจำลอง ANSYS เพื่อศึกษา
 พฤติกรรมของวัสดุพอลิเบนซอกซาซีนที่เติมสารตัดแปรสองชนิดข้างต้น คือ การกระจายความดัน
 และการสึกหรอ จากผลการทดลองจะได้ว่า เมื่อเติมถ่านแกนกัญชงลงไปพอลิเบนซอกซาซีนคอม
 พอสิตพบว่า สมบัติทางไทรโบโลยี สมบัติเชิงกลแบบไดนามิก สมบัติเชิงกลดีขึ้นอย่างมีนัยสำคัญ
 เนื่องจากถ่านแกนกัญชงยังคงมีส่วนที่เป็นลิกโนเซลลูโลสในโครงสร้าง ในขณะที่สมบัติทางความ
 ร้อน เช่น อุณหภูมิการสลายตัวทางความร้อนมีค่าลดลงเล็กน้อย เนื่องจากผงถ่านแกนกัญชงซึ่ง
 ยังคงมีโครงสร้างของลิกโนเซลลูโลสซึ่งมีอุณหภูมิการสลายตัวที่ต่ำกว่าแกรไฟต์สังเคราะห์ และจาก
 ผลการจำลองพบว่า การกระจายความดันจะเกิดขึ้นที่บริเวณขอบของคอมพอสิตมากที่สุด โดย
 เริ่มต้นพฤติกรรมการกระจายความดันจะกระจายจากบริเวณขอบมาที่บริเวณตรงกลาง แต่เมื่อ
 อุณหภูมิสูงมากขึ้นจะเกิดการกระจายความดันจากบริเวณขอบมาที่บริเวณตรงกลางน้อยลง ทำให้
 สามารถทำนายได้ว่าความดันบริเวณขอบของคอมพอสิตจะเพิ่มขึ้นตามการเพิ่มขึ้นของอุณหภูมิ
 นอกจากนี้การจำลองการสึกหรอของคอมพอสิตพบว่ามีค่าใกล้เคียงกับการสึกหรอที่ได้จากการ
 ทดลองโดยมีเปอร์เซ็นต์ของความผิดพลาดอยู่ในช่วงที่ยอมรับได้คือ 7เปอร์เซ็นต์

สาขาวิชา วิศวกรรมเคมี
 ปีการศึกษา 2562

ลายมือชื่อนิสิต
 ลายมือชื่อ อ.ที่ปรึกษาหลัก
 ลายมือชื่อ อ.ที่ปรึกษาร่วม

6170367621 : MAJOR CHEMICAL ENGINEERING

KEYWORD: POLYBENZOXAZINE, FRICTION MATERIALS, HEMP HURD, FRICTION
COEFFICIENT, WEAR SIMULATION

Nuttarika Kunaroop : Effects of Graphite/Partially Carbonized Hemp Hurd Particle Mass Ratios on Tribological Properties of Polybenzoxazine Composites. Advisor: Prof. SARAWUT RIMDUSIT, Ph.D. Co-advisor: Assoc. Prof. Chanchira Jubslip, D.Eng.

This work aims to study effects of friction modifiers, i.e., synthetic graphite and carbonized hemp hurd (CHH) on thermal stability, dynamic mechanical properties, mechanical properties, and tribological performances of polybenzoxazine-based friction composites. Simulation of brake pad and disc brake by using ANSYS simulation program to study behaviors of the friction modifier filled-polybenzoxazine composites, i.e. pressure distribution and wear rate was also investigated. The results show that when the CHH is added to the polybenzoxazine composites, the tribological, dynamic mechanical, and mechanical properties were significantly improved because of some lignocellulose structure of the partially CHH. While, thermal property i.e., thermal degradation slightly decreased because the degradation temperature of lignocellulose is lower than the degradation temperature of synthetic graphite. From the simulation, the maximum pressure distribution was at the edge of the composite. At the lower temperature region, the behavior of the pressure gradient of the composite was occurred from the edge to the middle. When increasing temperature, the pressure gradient toward the middle was decreased. Moreover, wear rates obtained from simulation were closed to the wear rate from experiment with an error in the range of 7% which is within acceptable tolerance.

Field of Study: Chemical Engineering

Student's Signature

Academic Year: 2019

Advisor's Signature

Co-advisor's Signature

ACKNOWLEDGEMENTS

This research was accomplished with cooperation from many parties. I would like to start by thanking my advisor: Prof. Dr. Sarawut Rimdusit and my co-advisor: Assoc. Prof. Dr. Chanchira Jubsilp for gave me a worth opportunity to do this research together with his suggestion, assistance, and observation including supporting throughout the course of this research.

This work has been supported by The National Research Council of Thailand (NRCT), Compact International (1994) Co., Ltd. (Thailand) for supported friction modifiers and fillers, PTT Phenol Company Limited. (Thailand) for supported Bisphenol A.

In addition, I am thankful to Polymer Laboratory, Department of Chemical Engineering, Faculty of Engineering, Chulalongkorn University for supporting the equipment and experiment locations, and Prof. Dr. Sanong Ekgasit, from Faculty of Science, Chulalongkorn University for supporting scanning electron microscope (SEM).

Finally, I have to express my grateful to my family and all my best friends for constant supporting, will power, advice, and kindly helps. Especially, Miss Pattarin Mora and Mr. Anun Wongpayakyotin. I would like to express my sincere thanks for their advice and efficient solution throughout the experiment.

จุฬาลงกรณ์มหาวิทยาลัย
CHULALONGKORN UNIVERSITY

Nuttarika Kunaroop

TABLE OF CONTENTS

	Page
ABSTRACT (THAI)	iii
ABSTRACT (ENGLISH)	iv
ACKNOWLEDGEMENTS	v
TABLE OF CONTENTS	vi
CHAPTER I INTRODUCTION	1
1.1 Introduction	1
1.2 Objectives	3
1.3 Scopes of the study	3
1.4 Procedure of the study	6
CHAPTER II THEORY AND LITERATURE REVIEW	7
2.1 Brake system	7
2.1.1 Drum brake	7
Drum brake	7
2.1.2 Disc brake	7
2.2 Brake pads ingredients	7
2.2.1 Binder	7
2.2.2 Reinforced fibers	9
2.2.3 Fillers	10
2.2.4 Friction modifier	11
2.3 Polybenzoxazine	11
2.4 Tribology	12

2.4.1 Friction coefficient	12
2.4.2 Wear rate	13
2.5 Thailand Industrial Standard (TIS97-2557)	14
2.6 Finite Element Analysis (FEA).....	16
2.6.1 Pre-processing.....	16
2.6.2 Analysis	17
2.6.3 Post processing.....	17
2.7 Euler Integration	17
2.8 Literature review.....	18
2.8.1 Experimental literature review.....	18
2.8.2 Simulation literature review	22
CHAPTER III EXPERIMENTAL	26
3.1 Materials and chemicals	26
3.2 Synthesis of benzoxazine resin.....	27
3.3 Sample preparation.....	27
3.4 Characterization.....	29
3.4.1 Thermogravimetric analyzer (TGA).....	29
3.4.2 Dynamic mechanical thermal analyzer (DMA).....	29
3.4.3 Universal testing machine.....	30
3.3.4 Tribometer.....	31
3.4.5 Constant speed friction testing machine	32
3.4.6 Worn surface morphology characterization of the samples.....	33
3.4.7 Simulations.....	33
CHAPTER IV RESULTS AND DISCUSSION.....	35

4.1. Dynamic mechanical thermal properties of graphite/carbonized hemp hurd-filled poly(BA-35x) composites.	35
4.2 Mechanical properties of poly(BA-35x) composites at various carbonized hemp hurd contents.	36
4.3 Thermal stability of synthetic graphite/carbonized hemp hurd-filled poly(BA-35x) composites at various carbonized hemp hurd contents.	37
4.4 Tribological properties of synthetic graphite/carbonized hemp hurd-filled poly(BA-35x) brake pad composites.	39
4.4.1 Coefficient of friction and wear rate of synthetic graphite/carbonized hemp hurd-filled poly(BA-35x) composites at room temperature (25°C). 39	
4.4.2 Coefficient of friction and wear rate of synthetic graphite/carbonized hemp hurd-filled poly(BA-35x) composites as a function of temperature.	42
4.5. Worn surface	44
4.6. Simulation of poly(BA-35x) friction composites filled with carbonized hemp hurd 8 wt% in the temperature range of 100-350 °C	46
CHAPTER V CONCLUSIONS	49
5.1 Conclusions	49
REFERENCES	50
VITA.....	57

CHAPTER I

INTRODUCTION

1.1 Introduction

Brake pad is one of the most important safety parts in automobiles. When brakes are applied with velocities, it causes the brake pads to touch the brake discs, which creates friction between the pads and discs; the friction causes heat and also resists the motion of the wheels and, therefore, slows down or stops the car [1]. In general, the ingredients of brake pads are classified to four classes: binders, reinforcing fibers, friction modifiers, and fillers. Binders are an important ingredient, which bind the composition integrity. Benzoxazine resin is one suitable candidate for this application because of its distinctive advantages that are suitable for employing as polymeric binders for non-asbestos organic friction materials (NAO FMs), including very low melt viscosity, good interfacial adhesion with fillers, self-polymerizability upon heating via ring-opening polymerization without catalyst or curing agent, and no by-product release in the curing process [2]. Polybenzoxazines also exhibit outstanding properties contributing to exceptional tribological performances of NAO FMs, including near-zero shrinkage, low water absorption, high glass transition temperature of 170 – 340 °C, high thermal stability with degradation temperature at 5% weight loss (Td5) of 315 – 350 °C, and excellent mechanical properties, i.e., flexural strength of 126 MPa and flexural modulus of 4.5 GPa [3-6]. Reinforcement fibers improve the mechanical properties and play a major role in maintaining stiffness, strength, and tribological behaviour of friction composites, fillers are added mainly to reduce cost and maintain the overall composition [7]. For friction modifiers, they are classified to abrasives and lubricants, which are desired friction characteristics. Frictional modifiers are ingredients added to friction materials in order to modify the friction coefficients as well as the wear rates, while solid lubricant, i.e. MoS₂, graphite, PTFE or starch is a material used as powder or thin film which reduces friction and wear of contacting surfaces in relative motion and provides protection from damage [8]. In recent years, friction polymer composites derived from natural and fast renewable resources, especially cellulosic materials, are developed due to eco-friendly nature and their numerous advantageous properties

such as low cost, availability, and sustainability [9, 10]. Natural fibers from hemp, flax, bamboo, jute, and coconut are increasingly considered as a good reinforcement material in friction polymer composites. Characteristics of natural fiber reinforced composite for brake pads material have been studied [11]. The authors reported that the composite reinforced with bamboo fibers has hardness of 37.14 HRB, friction coefficient of 0.454, and wear rate of 0.323 mm³/N.mm, while hardness, friction coefficient, and wear rate of the composite reinforced with coconut fibers was 44.10 HRB, 0.460, and 0.242 mm³/N.mm, respectively. To compare those properties of the composites with commercial brake pads, it was found that the hardness of the composites was lower than that of the commercial brake pad, while friction coefficient and wear rate of composites are relatively similar to the commercial one.

Hemp (*Cannabis Sativa* L.) is the source of two types of natural fibers: bast fibers (used mainly in the paper and textile industries) and woody core fibers —hurds. Hemp consists of approximately 20 wt% – 40 wt% of bast fibers and 60 wt% – 80 wt% of hurds. The hurds consist of 40–48 % cellulose, 18–24 % hemicellulose and 21–24 % lignin [12]. For hemp hurd, it has low density makes it useful as an absorbent, a filler for bricks, or for insulation (0.24–0.26 g/cm³). Hemp hurd may also be useful as a substitute for wood in wood/plastic composites. Hemp hurd contains slightly higher levels of cellulose and less lignin than wood, making it a potentially more effective reinforcing materials [13]. In addition, the enhancement of the mechanical performance of cement composites by the utilization of micro-sized carbonized hemp hurd particles was reported. The carbonized hemp hurd could act as a heterogenic obstacle in the way of crack tip and either forced it to deflect or to transform it into multiple cracks [14].

Therefore, in this work, effects of friction modifier mass content, i.e., synthetic graphite:carbonized hemp hurd on thermal, mechanical, and tribological properties of highly filled polybenzoxazine composites as friction materials were investigated. The mass contents of carbonized hemp hurd were varied at 0, 2, 4, 5, 6, 8 and 10 wt%. The thermal stability, dynamic mechanical properties and tribological properties of friction composite materials were measured by TGA, DMA, Universal testing machine and friction test, respectively.

Furthermore, this includes simulation in order to predict the behavior of the polybenzoxazine composite friction materials, using ANSYS and MATLAB program to simulate the contact pressure and wear rate of friction material by applying the Finite Element Analysis method. The simulation can provide insight into the deformation behavior thus helping reduce the time needed and cost of tribological tests.

1.2 Objectives

1.2.1 To evaluate the effects of carbonized hemp hurd particles on thermal, mechanical, and tribological properties of the obtained polybenzoxazine composites.

1.2.2 To simulate the wear rate of the polybenzoxazine composites by ANSYS and MATLAB program.

1.3 Scopes of the study

1.3.1 Synthesis of benzoxazine resin based on bisphenol-A, formaldehyde and aromatic amines 3,5-xylidine by solventless synthesis technology. The molar ratio of bisphenol A, paraformaldehyde, and 3,5-xylidine was 1:4:2. The three reactants were mixed at 110 °C for 40 min until the homogeneous mixture was obtained. Benzoxazine resin was solidified as a light yellow solid at room temperature. Finally, the solid monomer was ground to fine powder and kept in a refrigerator for future use.

1.3.2 Preparation of the aramid pulp and carbon fiber filled polybenzoxazine composites at aramid pulp: carbon fiber mass ratio of 75:25.

1.3.3 Preparation of Ingredient of benzoxazine composite.

(1) Thermal Binder is benzoxazine resin 10 wt%.

(2) Thermal Reinforcing fibers are iron fiber 25 wt% glass fiber 10 wt% and aramid pulp and carbon fiber 5 wt%.

(3) Thermal Fillers are barium sulphate 25 wt%, rubber dust 4 wt%, and cashew dust 4 wt%.

Glass fibers	10	10	10	10	10	10	10
Iron fibers	25	25	25	25	25	25	25
Barium sulfate	25	25	25	25	25	25	25
Acrylonitrile butadiene rubber (NBR)	4	4	4	4	4	4	4
Cashew dust	4	4	4	4	4	4	4

1.3.5 Study effect of carbonized hemp hurd particles on thermal, mechanical, and tribological properties of the obtained polybenzoxazine composites.

(1) Thermal properties are thermal degradation temperature and glass temperature which examined by using Thermal gravimetric analyzer (TGA) and Dynamic mechanical analyzer (DMA)

(2) Mechanical properties are flexural strength and modulus which examined by using Universal testing machine.

(3) Tribological properties are friction coefficient and specific wear rate which evaluated using a Constant speed test machine.

(4) Morphological properties worn surfaces obtained from sliding friction test examined by using a Scanning electron microscope (SEM).

1.3.6 Simulation wear rate of the polybenzoxazine composites by ANSYS and MATLAB program

(1) ANSYS

1) ANSYS Version 16.0

2) Velocity: 6 – 8 m/s

3) Rotor: 5000 revolutions

4) Pressure: 1 MPa

5) Poisson ration of composite brake pads

5) Young's modulus of composite brake pads

6) Friction coefficient of graphite/carbonized hemp hurd composite

(2) MATLAB

- 1) MATLAB (R2018a)
- 2) Archard's wear law
- 3) Euler integration

1.4 Procedure of the study

1. Reviewing related literature.
2. Preparation of chemicals and equipment to be used in this research.
3. Synthesis of benzoxazine resins by solvent less technique.
4. Preparation of benzoxazine composites.
5. Determination of thermal, mechanical and some tribological properties of benzoxazine composite as follows:
 - a. Coefficient of friction
 - b. Wear rate
 - c. Degradation temperature at 5 wt% loss ($T_{d,5}$)
 - d. Glass transition temperature (T_g)
 - e. Storage modulus
 - f. Flexural strength
 - g. Flexural modulus
6. Simulation and analysis of the experimental results.
7. Preparation of the final report.

CHAPTER II

THEORY AND LITERATURE REVIEW

2.1 Brake system

A brake system is designed to reduce and stop the movement of vehicle by converting kinetic energy into heat energy.

Friction is the resistance to movement exerted by two things. Two forms of friction play a part in controlling a vehicle: Kinetic or moving, and static or stationary. The amount of friction or resistance to movement depends upon the type of material in contact, the smoothness of their rubbing surfaces and the pressure holding them together. Brake classification is in terms of disc brake and drum brake. This refers to the mechanics of slowing down the vehicle [16].

2.1.1 Drum brake

Drum brake is a vehicle brake in which the friction is caused by a set of brake shoes that press against the inner surface of a rotating drum. The drum is connected to the rotating roadwheel hub. Just compared to disc brakes, drum brakes wear out faster due to their tendency to overheat [17].

2.1.2 Disc brake

Disc brake is a device for slowing or stopping the rotation of a road wheel. A brake disc usually made from cast iron or ceramic that connected to the wheel or the axle. To stop the wheel, friction material in the form of brake pads is forced mechanical. Friction causes the disc and attached wheel to slow or stop [17].

2.2 Brake pads ingredients

Brake pads typically comprise of the following subcomponents [18].

2.2.1 Binder

Binder which holds ingredients of a brake pad firmly. Among the ingredients in the friction material, polymer binders (especially thermosetting resin) owed a crucial role in determining the friction characteristics during braking [9]. Type of binder that is

used in the industry brake pads is phenolic resins which are widely used in the industry because it is cheap and easy to produce.

From **Table 2**, comparing the properties of binder, it was found that the benzoxazine resin has good properties more than other resin, such as high stability at high temperature and high flexural strength, etc.

Table 2 Properties of different binders [7].

Properties	Epoxy	Phenolics	PBA
Density (g/cm ³)	1.2 - 1.25	1.21 - 1.32	1.19
Max use temperature (°C)	180	200	130 - 280
Flexural strength (MPa)	90 - 120	24 - 45	127 - 148
Tensile modulus (GPa)	3.1 - 3.8	0.3-0.5	3.8 - 4.5
Elongation (%)	3 - 4.3	0.3	2.3 - 2.9
Dielectric constant (1 MHz)	3.8 - 4.5	04/10	3 - 3.5
Cure temperature (°C)	RT - 180	150 - 190	160 - 220
Cure shrinkage (%)	> 3	0.002	~ 0
TGA onset (°C)	260 - 340	300 - 360	380 - 400
T _g (°C)	150 - 220	170	170 - 340

From **Table 3**, comparing the properties of polybenzoxazines, it was found that the polybenzoxazine (BA- 35x) has good properties more than other polybenzoxazines, such as high stability at high temperature and high storage modulus, etc.

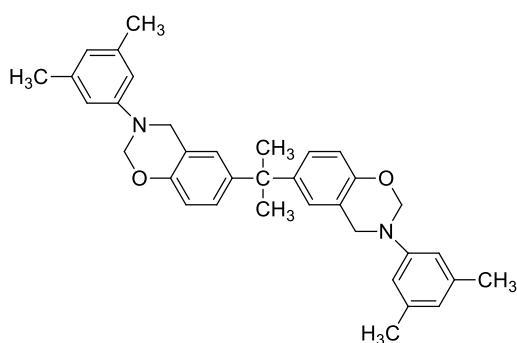


Figure 1 Polybenzoxazine (BA-35x) [18].

Table 3 Thermal and Mechanical Properties of the Polybenzoxazines [19].

Abbreviated Names	BA-a	BA-mt	Ba-35x
Amines used	aniline	m-toluidine	3,5-dimethylbenzene
T_g (°C)	168	209	238
T_d at 5% weight loss (°C)	315	350	350
Storage modulus at R.T. (GPa)	1.39	1.78	1.63
Storage modulus at rubbery plateau (MPa)	4.4	11.9	13.6
Molecular weight between crosslink	610	360	325
Crosslink density (mol/cm ³)	1.1×10^{-3}	1.9×10^{-3}	2.6×10^{-3}

2.2.2 Reinforced fibers

Reinforced fibers the purpose of reinforcing fibers is to provide mechanical strength to the friction material.

Table 4 Function of reinforced fibers [18].

Fiber	Function
Aramid	Good stiffness to weight ratio, excellent Soft, cannot be used without other fibers thermal resilience, good wear resistance
Carbon	High tensile strength, high thermal stability, good conductivity
Glass	High thermal stability (high melting Brittle point of 1430°C, but will start to soften at approximately 600°)
Metallic	Thermally resilient steel and copper have Large amounts may cause excessive rotor wear; melting points greater than 1000°C

2.2.3 Fillers.

Fillers in a brake pad are present for the purpose of improving its manufacturability as well as to reduce the overall cost of the brake pad [18].

Table 5 Function of fillers [18].

Filler	Function
Barium sulphate	Increase thermal stability
Cashew dust	Suppresses brake noise
Rubber dust	Suppresses brake noise

2.2.4 Friction modifier

Frictional modifiers are ingredients added to friction materials in order to modify the friction coefficients as well as the wear rates. They are ordered into two main groups: lubricants, which decrease the friction coefficients and wear rates, and abrasives, which increase friction coefficients and wear rates.

Table 6 Function of friction modifiers [18].

Friction modifier	Function
Graphite	Lubricants
Carbonized hemp hurd	Lubricants
Zirconium silicate	Abrasive

2.3 Polybenzoxazine

Polybenzoxazine is a new type of phenolic resin with interesting properties that are based on the ring opening polymerization of benzoxazine resin. Benzoxazine resin can be synthesized from low cost raw materials and can be cured without the catalyst. The resins can cross ring-opening polymerization without catalysts or curing agents and do not release by-products upon curing. The polybenzoxazine has good properties, such as high thermal stability, flame retardant, dimensional stability, low melt viscosity, near-zero shrinkage upon curing, low water absorption, high mechanical properties, glass transition temperature higher than cure temperature, fast mechanical property build-up as a function of degree of polymerization, high modulus, and high char-yield thus makes these polymers useful in many applications such as filled composites [20, 21]. The benzoxazine resins (BA-35x) is synthesized from Bisphenol A, Paraformaldehyde and 3,5-xylidine at 1:4:2 mole ratio by solvent less technology [15, 22].

2.4 Tribology

Tribology is basic of materials, surfaces, lubrication, and the interaction that determine the wear and frictional properties[23]. Tribology is motivated by mechanisms. They include most machine elements, from gears, bearings, clutches, and cables to human joints. The mechanisms are operated by impose loads, speeds, temperature, etc., on the rubbing elements or first bodies. Figure 2 presents the key elements of a tribological system.

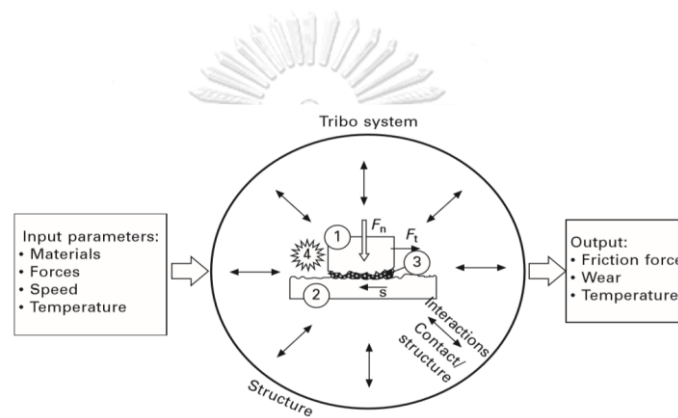
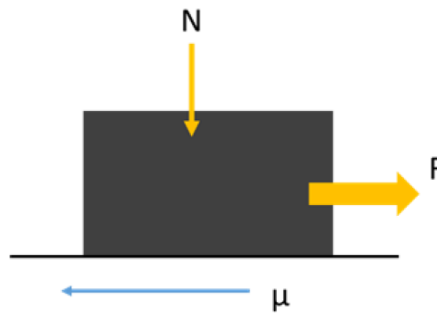


Figure 2 The various apparatuses of the tribological system: 1 and 2 are the two first bodies; 3 is the interfacial body or third body; 4 represents the environment [23].

2.4.1 Friction coefficient

Friction coefficient is the friction between two solid interfaces that is the resistance to tangential motion of one surface over the other, whether that motion is sliding, rolling, or rubbing contact. When two solid surfaces are brought into contact, adhesion can occur at the roughness between two solid surfaces, and this adhesive force at the interface types as a braking power. Normally there are two types of friction, static and kinetic. The rough surface will have more friction coefficient. Friction coefficient (μ) is calculated as follows in equation 1 [24, 25].

Equation 1 Friction coefficient (μ).



$$F = \mu N \quad (1)$$

Where μ is Friction coefficient

F is Force of friction (N)

N is Normal force (N)

2.4.2 Wear rate

Wear rate is strongly affected by the working conditions which are normal loads and sliding speeds. They play a pivotal role in determining wear rate [26]. Moreover, tribo-chemical reaction is also important for wear behavior. Different oxide layers are developed during the sliding motion [27]. The layers are originated from complex interaction among surface, lubricants, and environmental molecules. In general, a single plot, namely wear map. Demonstrating wear rate under different loading condition is used for operation. The specific wear rate (W_s) is calculated as follows in equation 2 [28].

Equation 2 Specific wear rate.

$$W_s = [(W_1 - W_2) \times \frac{10^2}{\rho}] / Pvt \quad (2)$$

where W_s is the specific wear rate ($\text{mm}^3/\text{N}\cdot\text{m}$)

W_1 is the weight before test (g)

W_2 is the weight after test (g)

ρ is the density of sample (g/cm^3)

P is the applied normal load (N)

v is the relative sliding velocity (m/s)

t is the experimental time (s)

Most wear models assume linearity, and they often assume that the wear is directly proportional to the local contact pressure. The most common wear model is named Archard's Wear Law. Although Holm formulated is the same model, It is much earlier than Archard. However, Archard and Holm interpreted the model differently. The model has followed equation 3 [29].

Equation 3 Archard's Wear Law.

$$V = K \cdot \frac{F_N}{H} \cdot S \quad (3)$$

Where V is the wear volume (mm³)

K is the dimensionless wear coefficient

F_N is the normal load (N)

S is the sliding distance (m)

H is the hardness of the softer contact surface

2.5 Thailand Industrial Standard (TIS97-2557)

Thailand Industrial Standard (TIS97-2557) had classified friction coefficient (COF) of brake pads, based on data shown in Table 7-11 [30].

Table 7 Classification of COF of brake pads [30].

Classification	Use
Class 1	Used only for parking brake those use for center brake, drum brake of drum in disc brake, etc.

Class 2	Drum brake use for light load
Class 3	Drum brake use for heavy load
Class 4	Used for disc brake

Table 8 Class 1 [30].

Item	Test temperature (°C)		
	100	150	200
Coefficient of friction	0.30-0.70	0.25-0.70	0.20-0.70
Wear rate (10^{-4} mm ³ /Nm)	1.0 or less	2.0 or less	3.0 or less

Table 9 Class 2 [30].

Item	Test temperature (°C)			
	100	150	200	250
Coefficient of friction	0.25-0.65	0.25-0.65	0.20-0.70	0.15-0.70
Wear rate (10^{-4} mm ³ /Nm)	0.5 or less	0.7 or less	1.0 or less	2.0 or less

Table 10 Class 3 [30].

Item	Test temperature (°C)				
	100	150	200	250	300
Coefficient of friction	0.25-0.65	0.25-0.70	0.25-0.70	0.20-0.70	0.15-0.70
Wear rate (10^{-4} mm ³ /Nm)	0.5 or less	0.7 or less	1.0 or less	1.5 or less	3.0 or less

Table 11 Class 4 [30].

Item	Test temperature (°C)					
	100	150	200	250	300	350
Coefficient of friction	0.25-0.65	0.25-0.70	0.25-0.70	0.25-0.70	0.25-0.70	0.25-0.70
Wear rate (10^{-4} mm ³ /Nm)	0.5 or less	0.7 or less	1.0 or less	1.5 or less	2.5 or less	3.5 or less

2.6 Finite Element Analysis (FEA)

Finite element analysis (FEA) is a numerical method used for the prediction of how a part or assembly behaves under given conditions. It is used as the basis for modern simulation software and helps engineers to find weak spots, areas of tension, etc. in their designs. The results of a simulation based on the FEA method are usually depicted via a color scale that shows for example the pressure distribution over the object. FEA involves solution of engineering problems using computers. Engineering structures that have complex geometry and loads, are either very difficult to analyze or have no theoretical solution. However, in FEA, a structure of this type can be easily analyzed. Commercial FEA programs, written so that a user can solve a complex engineering problem without knowing the governing equations or the mathematics; the user is required only to know the geometry of the structure and its boundary conditions. FEA software provides a complete solution including deflections, stresses, reactions, etc. The FEA consists of three steps: pre-processing, analysis, and post processing [31].

2.6.1 Pre-processing

Using a CAD program that either comes with the FEA software or provided by another software vendor, the structure is modeled. The final FEA model consists of several elements that collectively represent the entire structure. The elements not only represent segments of the structure, they also simulate mechanical behavior and

properties. Regions where geometry is complex (curves, notches, holes, etc.) require increased number of elements to accurately represent the shape; whereas, the regions with simple geometry can be represented by coarser mesh (or fewer elements). The selection of proper elements requires prior experience with FEA, knowledge of structure's behavior, available elements in the software and their characteristics, etc. The elements are joined at the nodes, or common points. In the pre-processor phase, along with the geometry of the structure, the constraints, loads and mechanical properties of the structure are defined. Thus, in pre-processing, the entire structure is completely defined by the geometric model. The structure represented by nodes and elements is called "mesh"[31].

2.6.2 Analysis

In this step, the geometry, constraints, mechanical properties and loads are applied to generate matrix equations for each element, which are then assembled to generate a global matrix equation of the structure [31].

2.6.3 Post processing

This is the last step in a finite element analysis. Results obtained in step 2 are usually in the form of raw data and difficult to interpret. In post analysis, a CAD program is utilized to manipulate the data for generating deflected shape of the structure, creating stress plots, animation, etc. A graphical representation of the results is very useful in understanding behavior of the structure [31].

2.7 Euler Integration

In mathematics there are several types of ordinary differential equations (ODE), like linear, separable, or exact differential equations, which are solved analytically, giving an exact solution. This means that there is a specific method to be applied in order to extract a general exact solution. One of the simplest integration methods is the Euler integration method, named after the mathematician Leonhard Euler. The Euler method is a first-order method, which means that the local error (error per step)

is proportional to the square of the step size, and the global error (error at a given time) is proportional to the step size.

The Euler integration method is also an explicit integration method, which means that the state of a system at a later time (next step) is calculated from the state of the system at the current time (current step) as shown in equation 4 [32].

Equation 4 Euler Integration [32].

$$y(t + \Delta t) = f(y(t)) \quad (4)$$

The Euler integration method is also called the polygonal integration method, because it approximates the solution of a differential equation with a series of connected lines (polygon).

2.8 Literature review

2.8.1 Experimental literature review

Kurihara et al. (2012) [33] had suggested the use of polybenzoxazine is binder in friction materials. They explained the case of a friction material using phenolic resin (PF) that showed the friction coefficient (COF) is no significant effect with material base on polybenzoxazine. The wear rate of phenolic resin material is lower than polybenzoxazine material in **Table12**. Moreover, friction material base on phenolic resin show a molding failure by cracking. The cracks generated during a curing step because it had ammonia gas by-product.

Table 12 Properties of friction material base on Phenolic and Benzoxazine [33].

Binder	COF	Wear rate (nm)
Phenolic (PF)	0.39	4.5
Benzoxazine (BZ)	0.41	3.7

W. Lertwassana et al. (2019) [34] develop aramid pulp/carbon fiber-reinforced polybenzoxazine composites as high performance friction materials. The effects of aramid pulps and carbon fibers on thermal stability, mechanical properties, and tribological performances of the composites were investigated. Aramid pulp/carbon fiber-reinforced polybenzoxazine composites exhibited high thermal stability with T_{d5} of 408–437 °C, high T_g of 240–265 °C, high mechanical properties, i.e. flexural strength of 57.2–79.4 MPa and flexural modulus of 10.2–21.4 GPa, high and stable coefficient of friction (COF), i.e. COF at 350 °C = 0.44, and high wear resistance, i.e. specific wear rate at 350 °C = 1.12×10^{-7} cm³/Nm. Coefficient of friction and friction stability could be improved by incorporating aramid pulps into the polybenzoxazine composites, while thermal stability, mechanical properties, dynamic mechanical properties including storage modulus and glass transition temperatures, and wear resistance could be enhanced by incorporating carbon fibers into the composites. The optimal aramid pulp:carbon fiber mass ratio for reinforcing polybenzoxazine composite was 75:25. Worn surfaces and wear debris after tribological testing of polybenzoxazine composites as investigated by scanning electron microscopy were in agreement with the observed specific wear rates, suggesting the combination of abrasive wear and adhesive wear mechanisms. Aramid pulp/carbon fiber reinforced polybenzoxazine composites could be potentially applied as high performance friction materials.

U.D. Idris et al. (2015) [35] develop new material for asbestos replacement as friction material and yet maintaining the same mechanical properties using agricultural waste (Banana peels). The surface of the agro-waste particles is smooth indicating that the compatibility between particles and the resin was good. It can be seen that the banana peels particles are not detached from the resin surface as the weight fraction of resin increased in the banana peels. The brake pad with BCp (Carbonized banana peels) formulation has a higher flame resistance than the BUNCp (Uncarbonized banana peels) formulation. This means that the BCp formulation increased the thermal decomposition temperatures and the residual yields of brake pad composite. This result indicated that the presence of BCp could lead to the

stabilization of the brake pad, resulting in the enhancement of the thermal stability. In the BCp brake pad composite, the BCp particles can effectively act as physical barriers to prevent the transport of volatile decomposed products out the brake pad composite during thermal decomposition. The wear mechanism reported was adhesion and delamination. The sample containing 25 wt% in BUNCp and 30 wt% BCp gave better properties than other samples tested. These grades of results were compared with that of commercial brake pad (asbestos based). The results are in close agreement. Hence asbestos free brake pad can be produced with these formulations. They indicate that banana peels particles can be effectively used as a replacement for asbestos in brake pad manufacture (shown in **Table 13**).

Table 13 Comparison of important properties between commercial brake pad and new laboratory formulation [35].

Properties	Commercial brake pad (asbestos based)	New laboratory formulation (carbonized banana peels)
Wear rate (mg/m)	3.80	4.67
Friction coefficient	0.30-0.40	0.35

B. Satapathy and J. Bijwe (2006) [36] discussed the sensitivity of friction and wear behavior of selected composites based on variation in the inclusion of organic fibres, viz., aramid, PAN, carbon, and cellulose, to braking pressure and sliding speed. The studies on the sensitivity of μ and wear to the operating variables have been carried out on a subscale brake-test-rig. Inclusion of cellulose fibre tended to increase the friction coefficient. The highest μ_m exhibited by cellulose based composite is primarily attributed to the shear induced degradation of the cellulose fibre via the weak β -glycoside linkages. This in turn caused faster damage of the composite surface that eventually leads to generation of large amounts of wear debris while aramid fibre improved the wear resistance. The aramid based composites, the interfacial friction

film rheology tended to be more shear thinning under severe pressure– speed conditions facilitating easier formation of sticky contact patches. The fibres of carbon and PAN made the friction composites least sensitive to dynamic variations in braking pressure and sliding speed that remained μ_m comparatively lower because of the inherent lubricity offered by these organic fibres (shown in **Figure 3**).

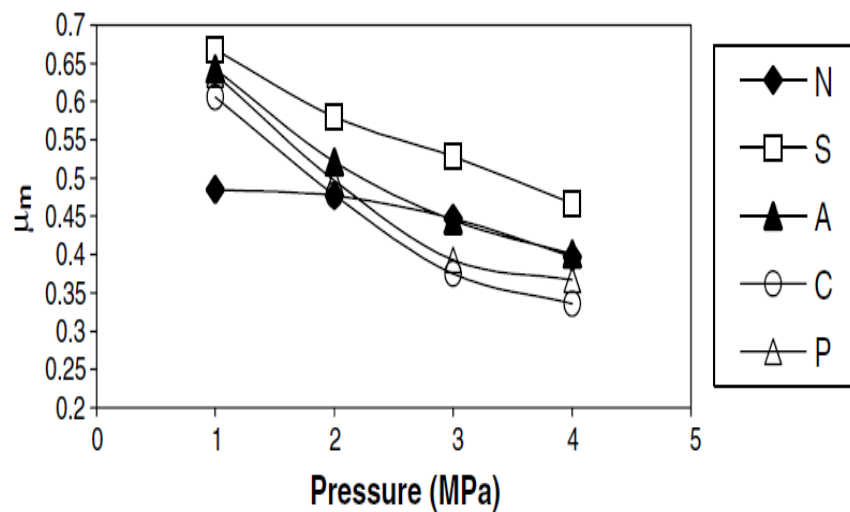


Figure 3 Variation in μ_m with increase in braking pressure at 12.6 m/s [31].

(N:with no organic fibre, A: with aramid fibre, P: with PAN fibre, C: with carbon fibre and S: with cellulose fibre)

I. Chukwujike, O. Jerome and G. Ihekwe (2015) [37] studied the influences of carbonized /uncarbonized corn hub powder on the vulcanizate properties of natural rubber/acrylonitrile butadiene rubber. The vulcanization properties of natural rubber/acrylonitrile butadiene rubber have been improved by using carbonized corn hub powder because during carbonization, some volatile materials are removed and also there is the removal of water of hydration which leads to improvement in mechanical properties. The carbonized corn-hub filled vulcanizates have higher modulus than uncarbonized filled vulcanizates and the abrasion resistance for carbonized corn hub filled vulcanizate was slightly higher than uncarbonized corn hub filled vulcanizate (shown in **Table 14**).

Table 14 The effects of Carbonized corn hub powder and Uncarbonized corn hub powder contents on the mechanical properties of natural rubber/ acrylonitrile rubber (NR/NBR) composite at different particle sizes [37].

Fillers	Mechanical Properties		
	Modulus (N/mm ²)	Hardness (IRAD)	Abrasion Resistance (%)
Carbonized corn hub powder (CCH)	2.3	62	41.8
Uncarbonized corn hub powder (UCCH)	1.54	49	41.5

2.8.2 Simulation literature review

A. Belhocine and W. Zaidi (2009) [38] investigated the structural and mechanical behavior of a three dimensional disc-pad model during the braking process under dry contacts slipping conditions. The predictive analysis is performed in order to determine the global deformations, Von Mises stress on the disc, and contact pressures on the inner and outer pad at different time of simulation. the contact pressure field at $t = 45$ s where the maximum pressures were reached at the end of the braking period. It found that the pressure distribution was almost identical in the three cases and it increased with the increase in the angular velocity of the disc. The location of the maximum pressure is located at the bottom loading edge pad. It observed that the increasing of pressure can create higher pad wear, and high pad wear could leave deposits on the disc. The maximum contact pressure in the pad is produced at the leading edge and trailing edge of the friction region. The distribution of frictional stress at time $t = 45$ s. It should be noted that the distribution of stress is symmetrical with respect to the pad groove and its value increases slightly when the rotational speed of the disc increases (shown in **Figure 4 and 5**).

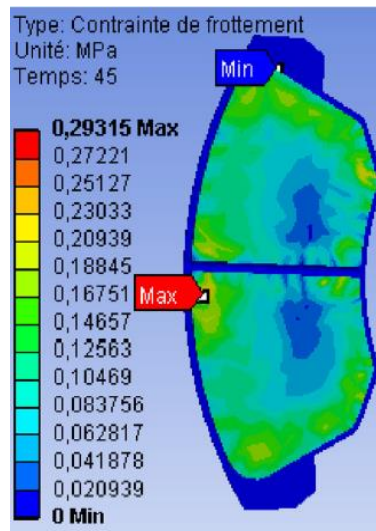


Figure 4 Interface friction stress distributions for different disc speeds [38].

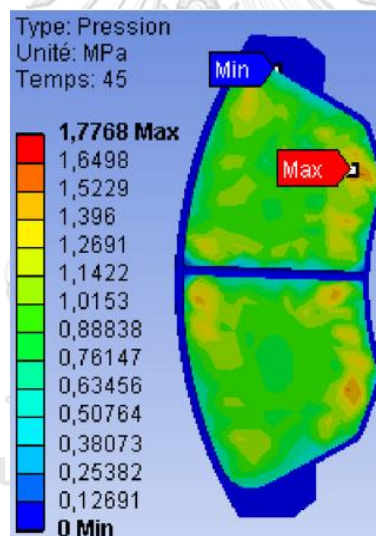


Figure 5 Interface contact pressure distributions for different disc speeds [38].

A. Soderberg and S. Andersson (2009) [39] discussed how general purpose finite element analysis software can be used to analyze the pad-to-rotor contact interface in passenger car disc brakes. A wear simulation routine has also been adopted in which the FE model is used to compute the pad-to-rotor pressure distribution. Based on the resulting distribution, the wear of the brake pad is computed using a generalized form of Archard's wear law and an explicit Euler integration scheme. The induced

frictional traction has shifted the pressure distribution toward the leading edge of the contact, leaving an open contact at the end. Looking at the surface profile we can see that the deepest wear occurs in the zone with high pressure, while there is almost wear at all at the edge. After the simulation is stopped the result is post-processed with a specially developed software package in the mathematical programming language MATLAB (shown in **Figure 6** and **7**).

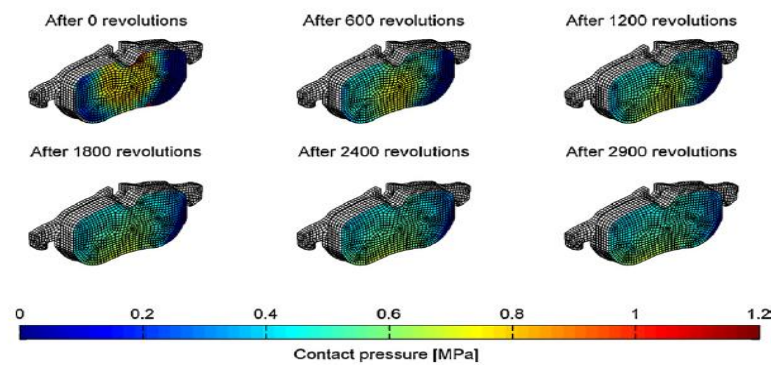


Figure 6 Pad-to-rotor pressure distribution for wear simulation with the prescribed rotor displacement [39].

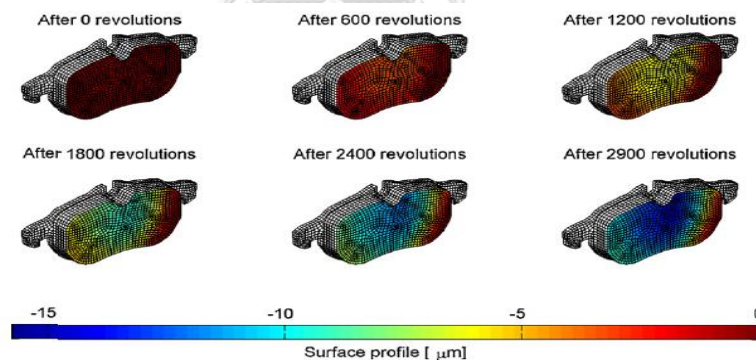


Figure 7 Surface profile of brake pad for wear simulation with the prescribed rotor displacement [39].

S.Zhang et al. (2019) [40] calculates the wear depth by considering the factors affecting wear. Based on the tribological principle of the high-power disc brake. The wear of the brake pad is a cumulative process, and the wear depth of the brake pad increases quickly and then slowly. The friction inlet and outlet edge regions of brake pad are extruded during braking, which is severely worn compared to the middle of the brake pad as shown in Figure 8.

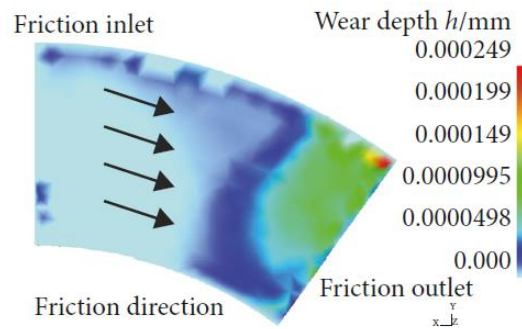


Figure 8 Nephogram of the brake pad wear depth [40].

The data points P1-P15 uniformly distributed on the brake pad are extracted from Figure 9. To clearly describe the wear condition of the brake pad, let points P1, P6, and P11 belong to the friction inlet region, and points P5, P10, and P15 belong to the friction outlet region point; the wear depth at the edge of friction inlet is relatively large. Because the friction intermediate region is far away from the friction edge and the pressing force is small, the material deformation is not obvious, and the friction heat is low, and then the wear degree is small.

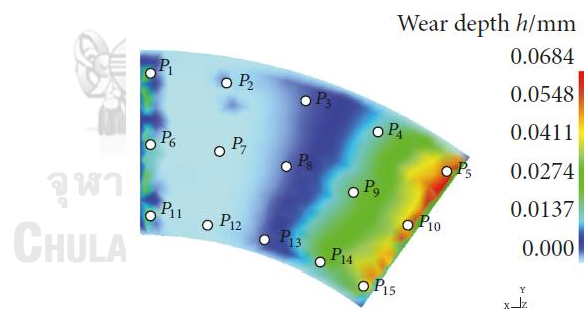


Figure 9 Nephogram of the brake pad point tracking [40]

CHAPTER III

EXPERIMENTAL

3.1 Materials and chemicals

- 3.1.1 Bisphenol A (AR grade)
- 3.1.2 Formaldehyde (AR grade)
- 3.1.3 3,5-Xylidine (AR grade)
- 3.1.4 Rubber dust
- 3.1.5 Aramid pulp (0.37 μm)
- 3.1.6 Carbon fiber (9.5 μm)
- 3.1.7 Glass fiber (16.4 μm)
- 3.1.8 Iron fiber (58 μm)
- 3.1.9 Zirconium silicate (3.3 μm)
- 3.1.10 Graphite powder (1.5 μm)
- 3.1.11 Carbonized hemp hurd powder (1.5 μm)
- 3.1.12 Barium sulfate (6.2 μm)
- 3.1.13 Cashew dust (23 μm)
- 4.1.14 ANSYS (Version 16.0)
- 4.1.15 MATLAB (R2018a)
- 4.1.16 SOLIDWORKS (Version 2014)

Bisphenol A (AR grade) was obtained from PTT Phenol Co., Ltd. (Bangkok, Thailand). Paraformaldehyde (AR grade) and 3,5-xylidine (AR grade) were purchased from Merck (Darmstadt, Germany) and Panreac Quimica S.A. (Barcelona, Spain), respectively. Aramid pulp was supported by DuPont, Japan. Carbon and glass fibers were purchased from SJ Sinthuphun Trading Co., Ltd, and Toho Beslon Carbon Co., Ltd, respectively. Steel fibers, friction modifiers and fillers were supplied by Compact International (1994) Co., Ltd. (Phetchaburi Thailand). Carbonized hemp hurd was supported by Highland Research and Development Institute (Public Organization) (Chiang Mai, Thailand).

3.2 Synthesis of benzoxazine resin.

Benzoxazine resin was synthesized using bisphenol A, paraformaldehyde, and aromatic amines with a molar ratio of 1:4:2 at 110°C for 40 minutes based on solvent less method disclosed in U.S. Patent 5,543,516 [41]. The benzoxazine resin obtained is a light-yellow solid which is then grounded to a fine powder and kept in a desiccator for future use.

3.3 Sample preparation.

The formulation of the composites is shown in **Table 15**. The molding compounds were mixed in internal mixer **Figure 8** (model MX105-D40L50 from Chareon Tut Co., Ltd. (Samutprakarn Thailand)) at 120°C for 45 mins. The compounds were then heated in a compression molder **Figure 9** (model LP20-B from Labtech engineering Co.,Ltd. (Bangkok Thailand)) at 200°C using a hydraulic pressure of 15 MPa for 2 hrs. The fully cured composites were cooled down to room temperature before characterizations.

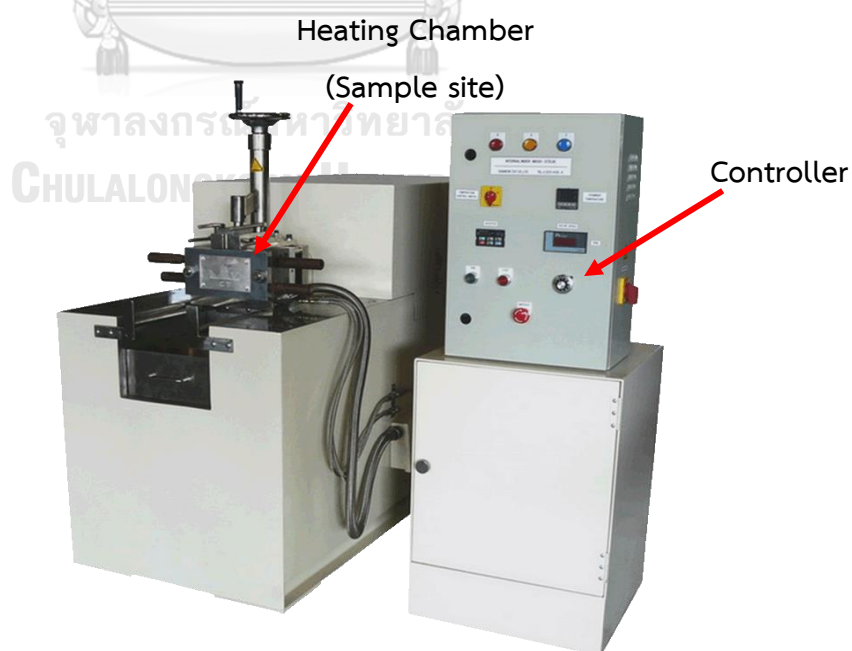
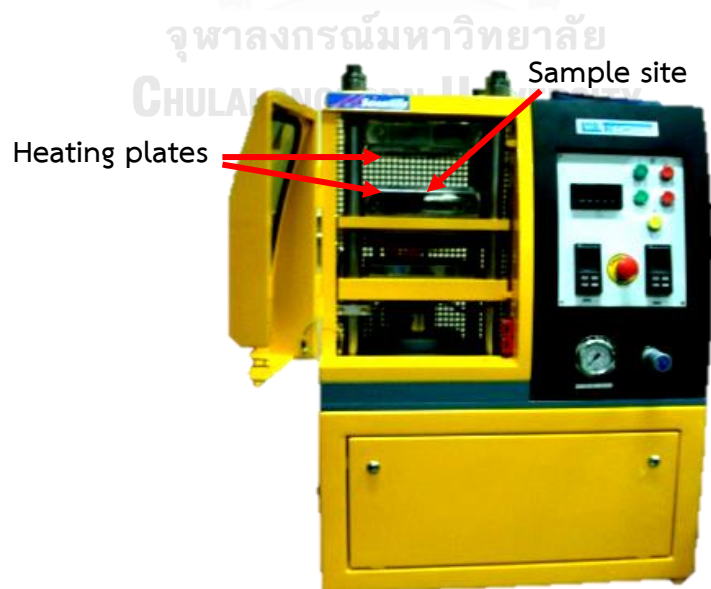


Figure 10 Internal mixer

Table 15 Formulation of composites for friction composite materials.

Constituent	Content (wt%)	Components
Benzoxazine resin	10	Binder
Aramid pulp	3.75	Fibers
Carbon fiber	1.25	
Glass fiber	10	
Iron fiber	25	
Graphite/Carbonized hemp hurd	10	Friction modifiers
Zirconium silicate	7	
Barium sulfate	25	Fillers
Rubber dust	4	
Cashew dust	4	

**Figure 11** Compression molder

3.4 Characterization

3.4.1 Thermogravimetric analyzer (TGA)

Degradation temperature (T_d) and char yield of the friction composite material were examined using a thermogravimetric analyzer (model TGA1 STARe System from Mettler-Toledo, (Thailand) Ltd. (Bangkok Thailand)). The initial mass of each tested specimen was 15-20 mg. Each specimen was heated from 30 to 1000 °C at a heating rate of 20 °C/min under nitrogen atmosphere. The degradation temperature at 5% weight loss and the char yield at 1000 °C were recorded.



Figure 12 Thermal gravimetric analyzer (TGA)

3.4.2 Dynamic mechanical thermal analyzer (DMA)

The dynamic mechanical analyzer (DMA) (model DMA1 STARe System from Mettler-Toledo, (Thailand) Ltd. (Bangkok Thailand)) was used to investigate the thermo dynamic mechanical properties. The dimension of specimens was 50 mm × 10 mm × 2.5 mm (W×L×T). The test was performed under three-point bending mode. The strain was applied sinusoidally at a frequency of 1 Hz. The temperature was scanned from 30 to 300°C with a heating rate of 2°C/min under nitrogen atmosphere. The storage modulus (E'), loss modulus (E''), and loss tangent or damping curve ($\tan \delta$) were then

obtained. The glass transition temperature (T_g) was taken as the maximum point on the $\tan \delta$ curve in the DMA thermograms.



Figure 13 Dynamic mechanical analyzer (DMA)

3.4.3 Universal testing machine

The flexural modulus and flexural strength of the friction composite material specimens were determined following ASTM D790-M93 using a universal testing machine, Instron, (model 5567 from Instron (Thailand) Co., Ltd. (Bangkok Thailand)). The dimension of each specimen was $25 \times 60 \times 3\text{mm}^3$. The test was performed in a three-point bending mode with a support span of 48 mm and at a crosshead speed of 1.2 mm/min. The flexural modulus and flexural strength were determined from the obtained load-displacement curve. Reported flexural strength and flexural modulus values were averaged from five specimens.

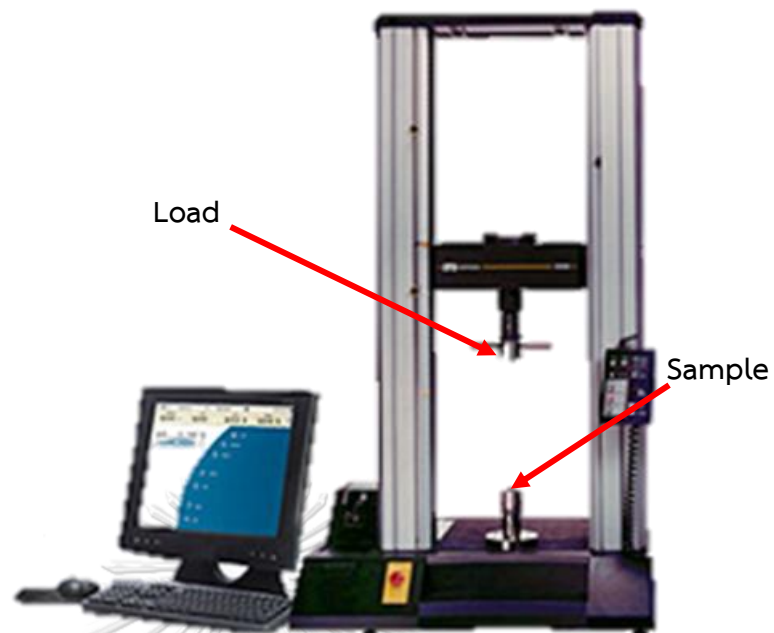


Figure 14 Universal testing machine (Instron model 5567)

3.3.4 Tribometer

This test was performed by a ball-on-disc tribometer (model CSM TRB-S-DE from Anton Paar Co., Ltd. (Bangkok Thailand)). In order to reproduce real operating conditions, a tungsten carbide was used as ball and the different composite formulations as discs. The cylindrical ball was 6 mm in diameter, the disc samples were 30 mm in diameter. The ball was assembled under the arm of the equipment applying a uniform load of 10 N against the surface of the sample disk, which rotated at a constant speed of 36.6 cm/s in the air. The total travel distance and the test time were respectively 1000 m. Specific wear rate of the friction composite materials was calculated.

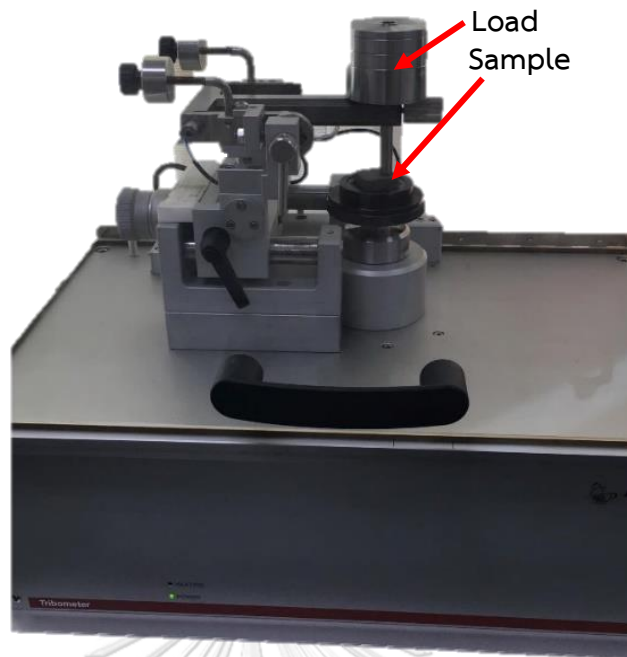


Figure 15 Tribometer (ball on disc)

3.4.5 Constant speed friction testing machine

Friction coefficients and wear rates of specimens as a function of temperature were determined from a constant speed brake lining tester (model HP-8-LC from Tokyo plant Co., Ltd. (Tokyo Japan)) at 100, 150, 200, 250, 300, and 350 °C, according to Japan Industrial Standard (JIS-D4411) [53]. The sample dimensions were 25 mm x 25 mm x 7 mm. The specific wear rate of the sample as a function of temperature was calculated from **Equation 5**.

Equation 5 Specific wear rate as a function with thickness [34, 42].

$$V = \frac{1}{2\pi R} \times \frac{A}{N} \times \frac{d_1 - d_2}{f_m} \text{ cm}^3 \text{ N}^{-1} \text{ m}^{-1} \quad (5)$$

where, V is specific wear rate (cm^3/Nm),

R is distance between the center of the tested specimen and the center of rotation axis (0.15 m),

N is total number of rotations of disc during the wearing test ($N= 5000$)

A is total frictional area of the tested specimen ($2.5\text{cm} \times 2.5\text{cm}$)

d_1 is average thickness of the specimen before testing (cm)

d_2 is average thickness of the specimens after testing (cm)

f_m is total average frictional force in testing (N).

3.4.6 Worn surface morphology characterization of the samples

Worn surfaces of samples were evaluated with a scanning electron microscope (SEM, model JSM-6510A from JEOL Ltd. (Tokyo Japan)) using an acceleration voltage of 5 kV. All samples were coated with a thin layer of gold film using a sputter coater (model SCD 040 from Oerlikon Balzers Coating (Thailand) Co. Ltd. (Chonburi Thailand)), making the worn surfaces conductive.

3.4.7 Simulations

(1) Wear rate simulation

The finite element code ANSYS 16.0 (3D) was used to simulate the behavior of the contact friction mechanism of the two bodies (brake pad and disc) during a braking stop. This code has the frictional contact management algorithms based on the Augmented Lagrange multipliers method. The simulations presented in this study, are considered the frictional pad to be deformable pad on a rigid disc. The brake pad was considered to be made of an isotropic elastic material [38]. The overall mechanical characteristics of the two parts was used in ANSYS program and wear behavior was calculated by MATLAB program from equation (6) - (8) [39].

$$h_{i,j} = h_{i,j-1} + \Delta h_{i,j} \quad (6)$$

$$\Delta h_{i,j} = kp_{i,j}\Delta s_{i,j} \quad (7)$$

where $h_{i,j-1}$ is the wear depth after the (j-1)th step,

$\Delta h_{i,j}$ is the incremental nodal wear depth during the jth step

$p_{i,j}$ is the nodal pressure

$\Delta s_{i,j}$ is the incremental nodal sliding distance

Equation 8 states that the incremental sliding distance of a node on the pad surface is proportional to its radial distance from the center of the rotor according to

$$\Delta s_{i,j} = n_j 2\pi r_i \quad (8)$$

where n_j is number of rotor revolutions during the j th step

r_i is number of rotor revolutions during the j th step.

(2) Absolute percentage error of Hyndman's MASE metric [43].

This is one of the measures used to evaluate forecasts using forecast errors. Forecast error is defined as actual observation minus forecast. The mean percentage error is the average or mean of all the percentage errors.

$$\text{Percentage error} = \frac{|X_{\text{Simulation}} - X_{\text{Experiment}}|}{X_{\text{Experiment}}} \quad (9)$$

Where $X_{\text{Simulation}}$ is simulation value

$X_{\text{Experiment}}$ is experimental value.

CHAPTER IV

RESULTS AND DISCUSSION

4.1. Dynamic mechanical thermal properties of graphite/carbonized hemp hurd-filled poly(BA-35x) composites.

Dynamic mechanical analysis is a widely used technique to determine thermal mechanical properties of the composites. The storage modulus (E') and loss modulus of friction materials as a function of temperature are listed in **Table 15**.

The storage modulus in glassy state of polybenzoxazine composite filled with carbonized hemp hurd contents of 0, 2, 4, 5, 6, 8, and 10 wt% were 4.93, 5.03, 5.18, 5.26, 5.42, 5.51, and 5.64 GPa respectively. The increase of storage modulus could be explained by the lignocellulosic structure was referred as a complex, three-dimensional, crosslinked, branched and heteropolymeric which ensures a strong chemical bond between the fiber and resin [44]. The storage modulus in the glassy state of benzoxazine composites can indicate the stiffness of friction composite.

Glass transition temperature (T_g) is the temperature at which the glassy behaviors of polymeric materials change to the rubbery ones upon heating. The thermal transition behaviors of thermosetting matrix have an effect on the wear performance of friction composite material [53]. The glass-to-rubber transition temperature of polybenzoxazine composites were determined from the maximum of $\tan \delta$. Glass transition temperature of poly(BA-35x) composites filled with carbonized hemp hurd contents of 0, 2, 4, 5, 6, 8, and 10 wt% were 212, 215, 218, 219, 222, 225, and 228 GPa respectively. The higher T_g value of polybenzoxazine composite material related to higher interfacial bonding between the fiber and polymer matrix leading to decrease in mobility of the macromolecules [45].

Table 15 Dynamic mechanical of synthetic graphite/carbonized hemp hurd-filled poly(BA-35x) composites at different carbonized hemp hurd contents.

Carbonized hemp hurd (CHH) (wt%)	Storage modulus (GPa)	T _g (°C)
0	4.93	212
2	5.03	215
4	5.18	218
5	5.26	219
6	5.42	222
8	5.51	225
10	5.64	228

4.2 Mechanical properties of poly(BA-35x) composites at various carbonized hemp hurd contents.

Flexural strength and flexural modulus of polybenzoxazine composites are shown in **Figure 16**. Both flexural strengths and flexural modulus values of the composites were increased with increasing carbonized hemp hurd contents from 0 to 10 wt%. The strength values were 43.2, 45.6, 46.9, 49.7, 50.0, 50.8, and 52.0 MPa, while the flexural modulus values were reported at 7.0, 7.7, 7.8, 8.1, 8.2, 8.4, and 9.0 GPa, respectively as shown in Figure xx. This may be due to remaining of strongly polar lignocellulose hydroxyl and carboxylic groups in carbonized hemp hurd which can be reacted with hydroxyl groups in poly(BA-35x). This behavior represents one of the significant load transfers, which contribute to the high modulus values of the composite materials [46]. In addition, the flexural properties of our composite systems are higher value than the normal range reported for friction materials, i.e., flexural strength of 10.0-40.0 MPa and flexural modulus of 3.0-8.0 GPa [47].

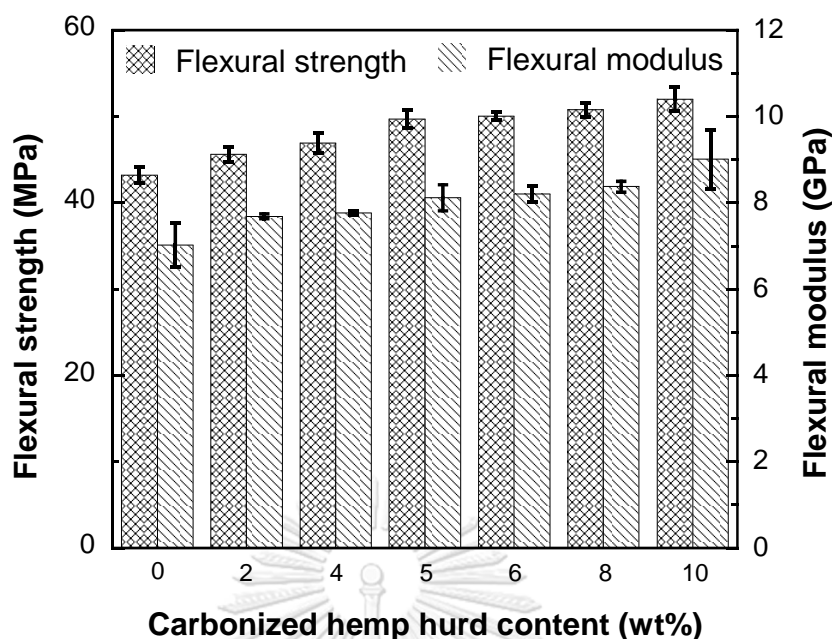


Figure 16 Flexural strength and modulus of poly(BA-35x) composites at various carbonized hemp hurd contents.

4.3 Thermal stability of synthetic graphite/carbonized hemp hurd-filled poly(BA-35x) composites at various carbonized hemp hurd contents.

In **Figure 17**, TGA thermograms of synthetic graphite/carbonized hemp hurd-filled poly(BA-35x) composites were performed to determine the thermal stability of poly(BA-35x) composite at different carbonized hemp hurd (CHH) contents by analyzing the degradation temperature at five percent weight loss (T_{d5}) and residual weight at 1000 °C. There were three main degradation steps detected in the TGA thermograms of the composites as shown in Figure. The first degradation step was found in the range of 250-500 °C corresponding to the degradation of lignocellulose, cashew dust, NBR powder and benzoxazine resin. The decomposition of hemicellulose, cellulose and lignin occurred at ranges of 180-240, 230-310, and 300-400 °C, respectively [48]. The second degradation step presented the onset temperature from 500 °C to 600 °C displaying the degradation of aramid pulp. The onset and offset temperatures of third degradation step were observed at approximately 600 °C and 900 °C, respectively, presenting degradation of barium sulphate and lignocellulose [34].

The T_{d5} of friction composite materials decreased with the addition of CHH. The T_{d5} of the poly(BA-35x) composites showed the maximum value of 420 °C at synthetic graphite of 10 wt%, while addition of CHH at 2 wt%, 4 wt%, 5 wt%, 6 wt%, 8 wt% and 10 wt% provided the T_{d5} values of 418 °C, 415 °C, 413 °C, 411 °C, 409 °C and 404 °C, respectively. It can be seen that the T_{d5} of the poly(BA-35x) composites tended to decrease with the addition of CHH. Furthermore, the residual weight at 1000 °C of the poly(BA-35x) composites also decrease with increasing CHH contents. The values of residual weight at 1000 °C were in the range of 71.5–73.7%. This behavior is possible due to that some lignocellulose structure still remains in the CHH which starts to degrade at relatively low temperature of 200–275 °C [49]. However, the T_{d5} value of synthetic graphite/carbonized hemp hurd-filled poly (BA-35x) composites exhibited higher values than that of the phenolic composites (commercial product), i.e. 402 °C and 63%, respectively.

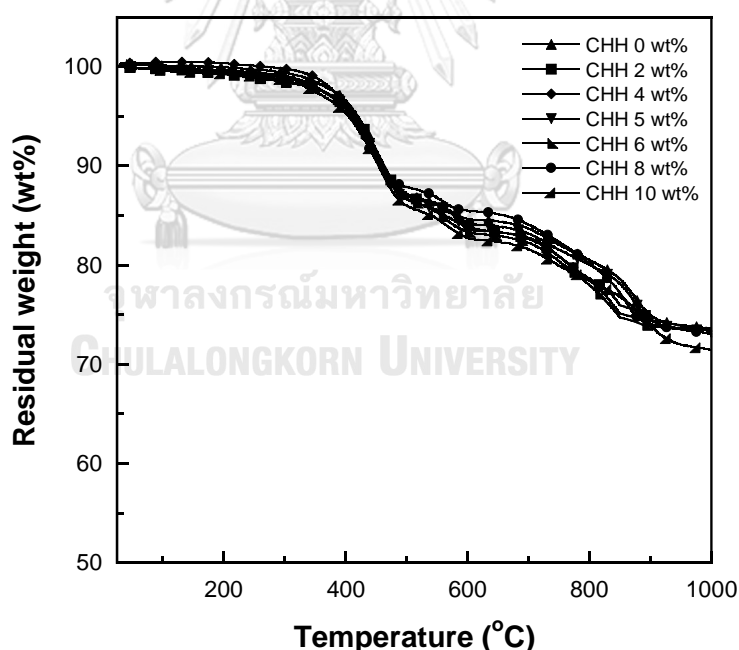


Figure 17 TGA thermogram of TGA thermograms of synthetic graphite/carbonized hemp hurd-filled poly(BA-35x) composites at various carbonized hemp hurd contents.

Limiting Oxygen Index (LOI) is the minimum percentage of oxygen it takes in an air-like gas mixture to support flaming combustion [50]. In **Table 16**, LOI could be calculated from Residual weight as indicated in this equation by using the Residual weight at 1000 °C. The LOI of the poly(BA-35x) composites also decrease with increasing CHH contents but LOI value of polybenzoxazine friction composites exhibited higher values than the commercial brake pads that causes the flame-retardant of polybenzoxazine friction composites is higher than the commercial brake pads.

Table 16 Limiting Oxygen Index (LOI) of synthetic graphite/carbonized hemp hurd-filled poly(BA-35x) composites at different carbonized hemp hurd contents.

Carbonized hemp hurd (CHH) (wt%)	LOI
0	46.88
2	46.80
4	46.76
5	46.72
6	46.64
8	46.53
10	46.00

4.4 Tribological properties of synthetic graphite/carbonized hemp hurd-filled poly(BA-35x) brake pad composites.

4.4.1 Coefficient of friction and wear rate of synthetic graphite/carbonized hemp hurd-filled poly(BA-35x) composites at room temperature (25°C).

Tribological properties are the key parameter for friction material. Tribological responses and performances of friction materials could be evaluated through coefficient of friction and wear rate [51].

Figure 18 and **Table 17** show the relationship between coefficient of friction and sliding distance of synthetic graphite/carbonized hemp hurd-filled poly(BA-35x) brake pad composites. These reported COF values were determined by averaging coefficient of friction values within the sliding distance of 200–1000 m. The coefficient of friction values at room temperature of brake pad composite filled with carbonized hemp hurd contents of 0, 2, 4, 5, 6, 8, and 10 wt% were 0.30, 0.31, 0.32, 0.33, 0.34, 0.36, and 0.38 respectively. Coefficient of friction of polybenzoxazine composites increased with increasing carbonized hemp hurd contents. This might be due to enhanced carbonized hemp hurd contents in polybenzoxazine composites leading to decreased stress absorbing capacity of the composites related to the increase of friction coefficient at room temperature [36].

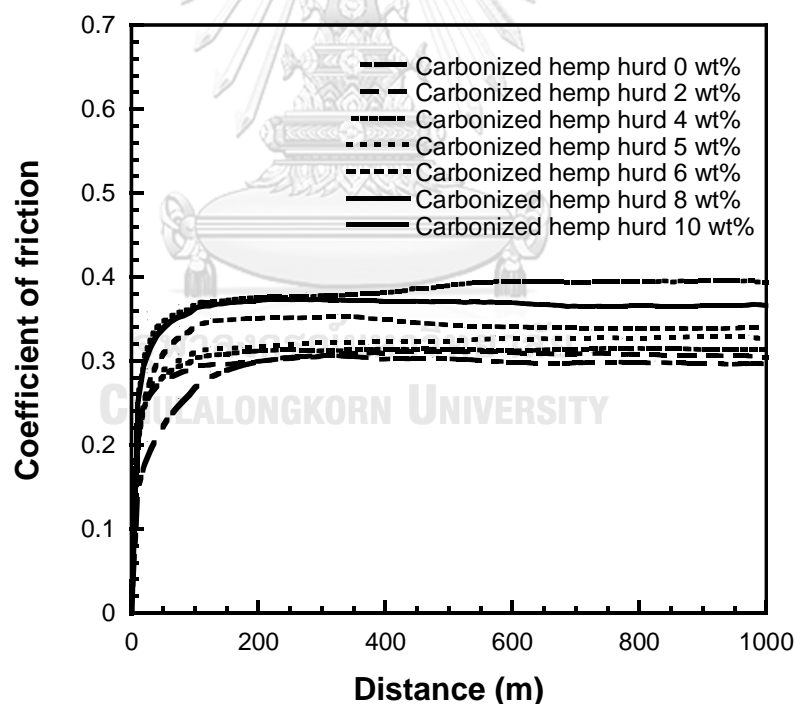


Figure 18 Coefficient of friction of synthetic graphite/carbonized hemp hurd-filled poly(BA-35x) composites at various carbonized hemp hurd contents.

Table 17 show the wear rate of synthetic graphite/carbonized hemp hurd-filled poly(BA-35x) composites. Wear rate values at room temperature of brake pad composite filled with carbonized hemp hurd contents of 0, 2, 4, 5, 6, 8, and 10 wt% were 1.36, 1.52, 1.84, 2.17, 2.58, 2.87, and 3.57 cm³/Nm respectively. The wear rates of polybenzoxazine brake pad composite increased with increasing carbonized hemp hurd contents in polybenzoxazine composites. This might be due to enhanced carbonized hemp hurd contents of polybenzoxazine composites leading to decreased thermal degradation of composites related to increased wear rate at room temperature[52]. It also affected the overall integrity of the composite adversely causing the surface damage and debris detachment easier [36].

Table 17 Friction coefficient and wear rate of synthetic graphite/carbonized hemp hurd-filled poly(BA-35x) composites at different carbonized hemp hurd contents.

Carbonized hemp hurd (CHH) (wt%)	Friction coefficient	Specific wear rate (10 ⁻⁷ cm ³ /Nm)
0	0.30±0.01	1.36±0.09
2	0.31±0.00	1.52±0.07
4	0.32±0.03	1.84±0.16
5	0.33±0.01	2.17±0.14
6	0.34±0.01	2.58±0.30
8	0.36±0.02	2.87±0.06
10	0.38±0.02	3.57±0.13

4.4.2 Coefficient of friction and wear rate of synthetic graphite/carbonized hemp hurd-filled poly(BA-35x) composites as a function of temperature.

The coefficient of friction of the polybenzoxazine composite as a function of temperature from 100 °C to 350 °C was investigated based on Thailand industrial standard (TIS : 97-2014) [30]. From the previous results the composite filled with carbonized hemp hurd contents of 8 wt% was selected for the test because its friction coefficient under 100 °C of 0.36 being in the range of 0.35 - 0.45 as industrial standard for brake pads of personal car [53].

Figure 19 shows coefficients of friction of synthetic graphite/carbonized hemp hurd-filled polybenzoxazine composites as a function of temperature. COF values of the polybenzoxazine composite filled with carbonized hemp hurd contents of 8 wt% were 0.38, 0.36, 0.36, 0.35, 0.37, and 0.38 when the tested temperatures were 100, 150, 200, 250, 300, and 350 °C, respectively. The COF values of the polybenzoxazine composites remained relatively constant with increasing temperatures. The maintainability of COF values of the polybenzoxazine composites in the temperature range of 250–350 °C implied that the real contact area between the friction pair was increased. This was attributed to the glassy-to-rubbery transition of the polybenzoxazine composite at $T_g = 244$ °C. At the rubbery state, the storage modulus of polybenzoxazine composite drastically decreased and the composite could be deformed easily, increasing the real contact area between the composite and the rigid asperity [52]. The COF value at 350 °C of our synthetic graphite/carbonized hemp hurd-filled polybenzoxazine composite, i.e. COF 0.38, exhibited a higher value than those of the ceramic-matrix friction materials with mixing steel fiber and mullite fiber, i.e. COF at 350 °C = 0.37 [42], the nanocomposite friction materials employing phenolic resin as binder, i.e. COF at 350 °C = 0.34 [54], and the Akebono brake pads composites, i.e. minimum COF is 0.28 [55].

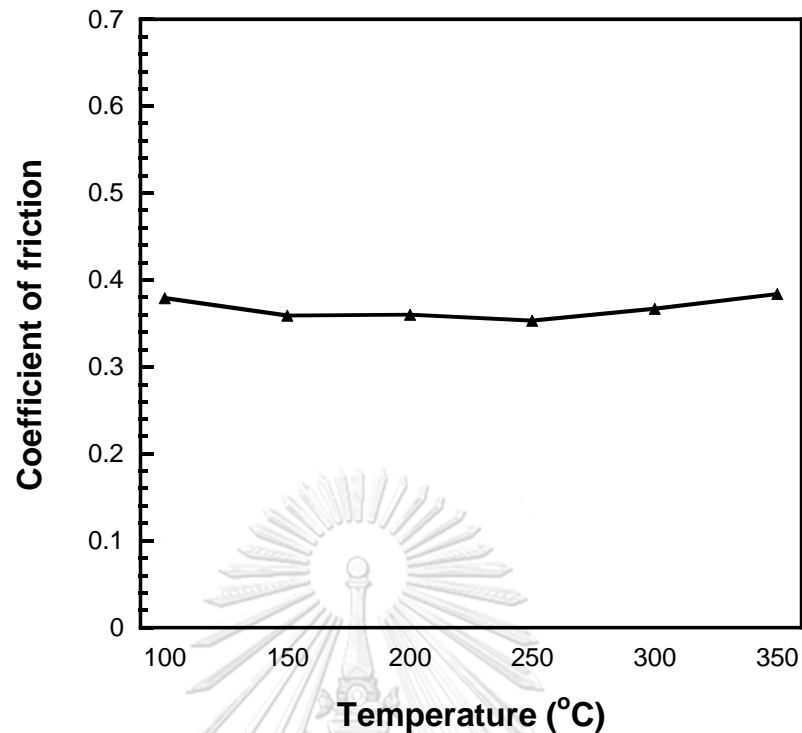


Figure 19 Coefficient of friction composite filled with carbonized hemp hurd contents of 8 wt% as a function of temperature.

Figure 20 shows specific wear rate of the synthetic graphite/carbonized hemp hurd-filled polybenzoxazine composite as a function of temperature. Specific wear rates of the polybenzoxazine composite filled with carbonized hemp hurd contents of 8 wt% at the tested temperatures of 100, 150, 200, 250, 300, and 350 °C were 0.16×10^{-7} , 0.16×10^{-7} , 0.17×10^{-7} , 0.26×10^{-7} , 0.29×10^{-7} and 0.39×10^{-7} cm^3/Nm , respectively. Specific wear rates of the composites increased with increasing temperature. Our results showed similar trends with the reported work of Oztürk et al. [56]. Specific wear rates of the polybenzoxazine composites dramatically increased when the tested temperatures were changed from 200 to 300 °C. The polybenzoxazine composite could be deformed easily at the glassy-to-rubbery transition within the tested temperature range, strengthening the interlocking between the contact pairs and increasing the specific wear rates [52]. The specific wear rate of the polybenzoxazine composite at the tested temperature of 350 °C was also drastically increased to

$0.39 \times 10^{-7} \text{ cm}^3/\text{Nm}$ because of the thermal degradation of poly(BA-35x) binder, weakening the bond strength between the resin binder and various components of the composite [56, 57]. Specific wear rate at 350 °C of our synthetic graphite/carbonized hemp hurd-filled polybenzoxazine composite, i.e. specific wear rate of $0.39 \times 10^{-7} \text{ cm}^3/\text{Nm}$, exhibited a lower value than those of the ceramic-matrix friction materials with mixing steel fiber and mullite fiber, i.e. specific wear rate at 350 °C of $1.30 \times 10^{-7} \text{ cm}^3/\text{Nm}$ [69], and the nanocomposite friction materials employing phenolic resin as binder, i.e. specific wear rate at 350 °C of $1.18 \times 10^{-7} \text{ cm}^3/\text{Nm}$ [54].

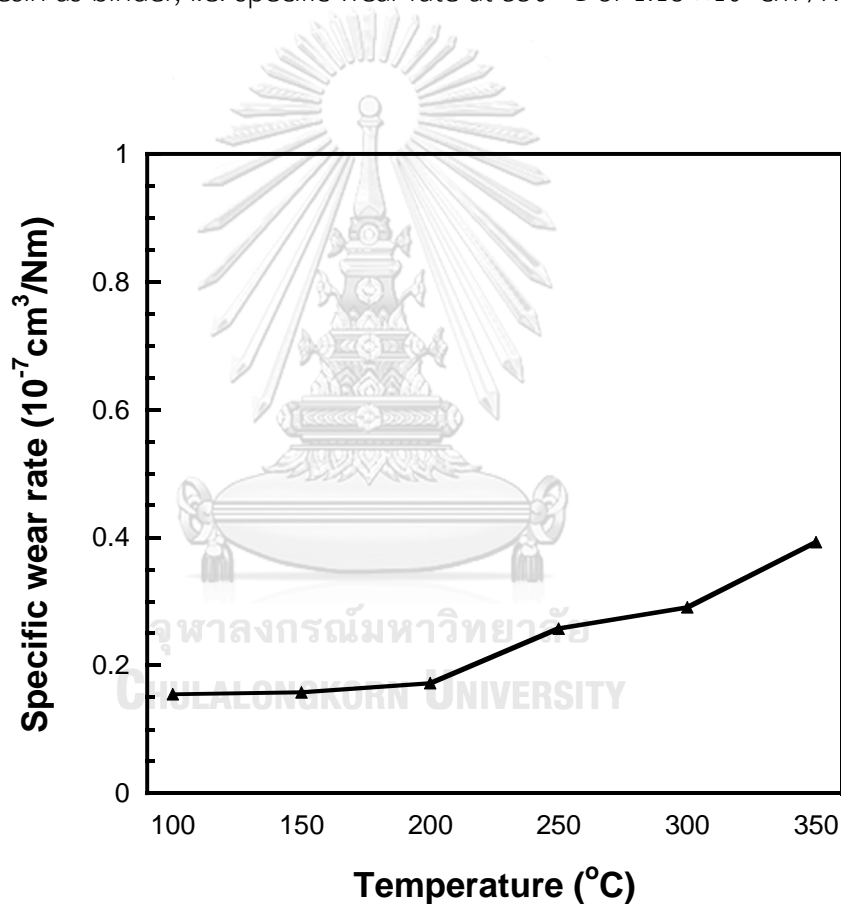


Figure 20 Specific wear rate of friction composite materials as a function of temperature.

4.5. Worn surface

Worn surfaces of friction materials after tribological tests are utilized for investigating wear mechanism [58]. Worn surfaces are related to friction coefficient and wear rate

of friction materials [59]. Worn surfaces of the specimens were analyzed by scanning electron microscopy.

Figure 21 shows worn surfaces of polybenzoxazine friction composites at various carbonized hemp hurd after tribological tests at room temperature. Cracks and small grooves were observed on worn surfaces of **Fig. 21A**, implying abrasive wear mechanism [51]. In addition, small cracks perpendicular to the sliding direction were also observed on surfaces of friction composites after an addition of carbonized hemp hurd (**Fig. 21B–C**). Cracks and small grooves on worn surfaces of polybenzoxazine friction composites were increased when carbonized hemp hurd contents in polybenzoxazine composites increased, leading to enhanced wear of composite. The wear of friction composites filled with CHH 10 wt% was dramatically increased that support trend of the wear rate in previous testing.

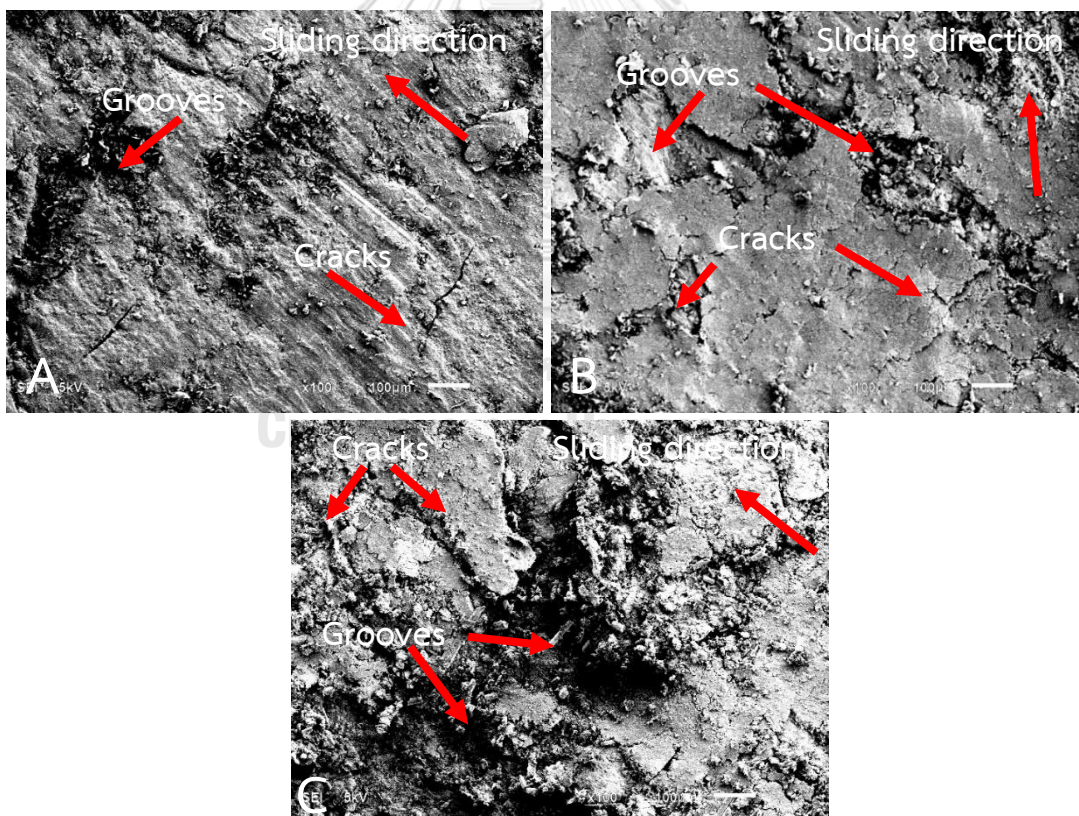


Figure 21 SEM micrographs of wear debris of polybenzoxazine friction composites at various carbonized hemp hurd contents: (A) 0 wt%, (B) 8 wt%, (C) 10 wt%

4.6. Simulation of poly(BA-35x) friction composites filled with carbonized hemp hurd 8 wt% in the temperature range of 100-350 °C

The structural boundary conditions of the pad of synthetic graphite/carbonized hemp hurd-filled poly(BA-35x) friction composites as tabulated in Table 18 were applied for finite element analysis simulation. From simulation results, the finite element analysis simulation contour of contact pressure of poly(BA-35x) filled with CHH 8 wt% composites at 100-350 °C was listed in **Table 19** and the visual appearance of the interface contact pressure distribution on poly(BA-35x) friction composites filled with 8 wt% of carbonized hemp hurd at 350 °C is shown in **Figure 22** (the visual appearances of the interface contact pressure distribution of the composite at 100-250 °C was similar to the composite at 350 °C and they are not shown here). It was observed that the pressure distribution of the composite tended toward the leading edge of the contact. From Table 19, the wear rates of the composites were increased with increasing maximum pressure values related to temperature. The maximum pressure occurred at the edge of friction material is relatively large. Due to the majority of the pressing force being applied at the edge, the intermediate region of the friction material is not affected much; therefore, the deformation to the material is not obvious at a glance and not much heat generated from friction is accumulated which also corresponded to a lower wear degree. Comparing the longitudinal distribution of simulation results, the outer region of the friction inlet wear value was larger than those of the middle region results. The wear depth at the friction outlet increases from the inner circle region to the outer circle region because the outer circle region has a higher frictional line speed than the inner circle region and the higher temperature of the outer circle region; therefore, the larger corresponding wear. Comparing the lateral distribution of the simulation, there is large wear at the friction outlet (right hand side of brake pad) [40]. From the simulation, the wear rate of friction composite compared with the wear rate of friction composite from experiment showed the error about 6- 7% which is within acceptable tolerance [60, 61].

Table 18 The structural boundary conditions applied to the pad of synthetic graphite/carbonized hemp hurd-filled poly(BA-35x) friction composites.

Conditions	Pad
Pressure of piston pad (MPa)	1
Friction coefficient	0.35-0.38
Constant angular velocity (rad/s)	46.67
Simulation time for braking (s)	673
Mesh	tetrahedral 3D elements
Formulation	Augmented Lagrange
Relevance	100
Fixed support	finger pad
Temperature	100-350 °C
Wear coefficient (Pa ⁻¹)	$1.55 \times 10^{-14} - 2.17 \times 10^{-13}$
Revolutions (rounds)	5,000
Radius (m)	0.15
Increment of initial time (s)	0.25
Increment of minimal initial time (s)	0.125
Increment of maximal initial time (s)	0.5

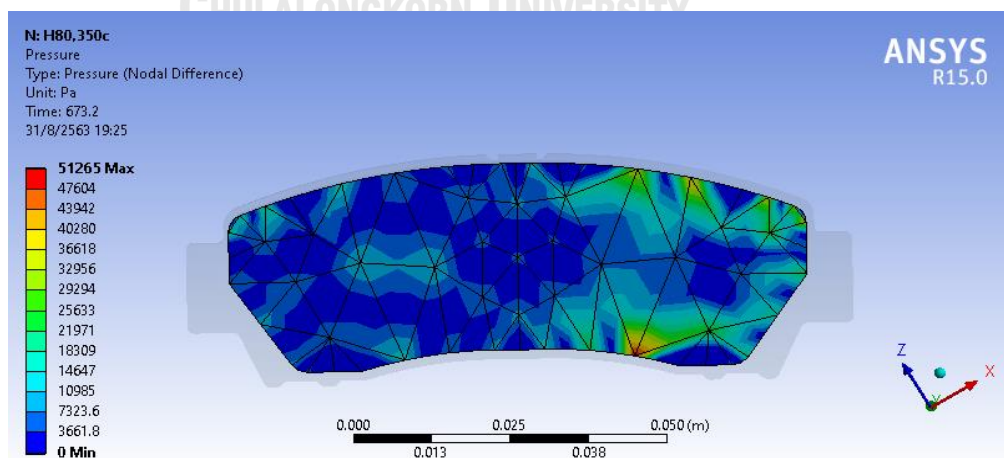


Figure 22 Interface contact pressure distribution on poly(BA-35x) friction composites filled with 8 wt% of carbonized hemp hurd at 350 °C

Table 19 Wear rate on the pad of synthetic graphite/carbonized hemp hurd-filled poly(BA-35x) friction composites and this work simulation.

Temperature (°C)	Friction coefficient	Maximum pressure (10 ⁴ Pa)	Wear rate from experiment (10 ⁻⁷ cm ³ /Nm)	Wear rate of simulation (10 ⁻⁷ cm ³ /Nm)	%error
100	0.38	5.15	0.15	0.14	6%
150	0.36	5.00	0.16	0.14	9%
200	0.36	5.05	0.17	0.16	8%
250	0.35	5.17	0.26	0.24	6%
300	0.37	5.11	0.29	0.27	7%
350	0.38	5.13	0.39	0.37	7%

CHAPTER V

CONCLUSIONS

5.1 Conclusions

Friction composite materials from poly(BA-35x) composite filled with varying carbonized hemp hurd contents (0, 2, 4, 5, 6, 8, 10 %wt) with excellent thermal stability, mechanical properties, dynamic mechanical properties, and tribological properties were successfully developed. Friction composite materials exhibited high thermal stability with T_{d5} of 404-420 °C, high T_g of 212–228 °C, high mechanical properties, i.e. flexural strength of 43.2-52.0 MPa and flexural modulus of 7.0-9.0 GPa, high and stable coefficient of friction (COF), i.e. COF at 350 °C = 0.38, and high wear resistance, i.e. specific wear rate at 350 °C = $0.39 \times 10^{-7} \text{ cm}^3/\text{Nm}$. From the experiment, it can be concluded that the higher lignocellulose structure resulted in higher mechanical properties, higher friction coefficient and lesser wear rate with good properties of friction materials (high friction coefficient and low wear rate). The polybenzoxazine composite filled with 8 wt% possessed superior properties suitable for use as friction materials and wear rate obtained from simulation were close in values to the wear rate from experiment at different temperatures with an error in the range of 7% which is within acceptable tolerance.

REFERENCES

1. Dante, R., *Handbook of Friction Materials and their Applications 1st Edition*. 2016, United Kingdom: Elsevier Ltd.
2. Ishida, X.N.a.H., *Phenolic materials via ring-opening polymerization: synthesis and characterization of bisphenol-A based benzoxazines and their polymers*. *Journal of Polymer Science: Part A: Polymer Chemistry*, 1994. **32**(6): p. 1121-1129.
3. Jantaramaha, J., C. Jubsilp, and S. Rimdusit, *Thermal and Mechanical Properties of Acrylonitrile-Butadiene Rubber Modified Polybenzoxazine as Frictional Materials*. *Key Engineering Materials*, 2015. **659**: p. 511-515.
4. Taewattana, R., et al., *Effect of gamma irradiation on properties of ultrafine rubbers as toughening filler in polybenzoxazine*. *Radiation Physics and Chemistry*, 2018. **145**: p. 184-192.
5. Allen, H.I.a.D., <*Physical and Mechanical Characterization of Near-Zero Shrinkage Polybenzoxazines.pdf*>. *Journal of Polymer Science: Part B: Polymer Physics*, 1996. **34**(6): p. 1019-1030.
6. Agag, H.I.a.T., *Handbook of benzoxazine resins 1st Edition*. 2011, Amsterdam: Elsevier.
7. Bijwe, J., *Multifunctionality of nonasbestos organic brake materials*. *Multifunctionality of Polymer Composites*. 2015.
8. Bart, J.C.J., E. Gucciardi, and S. Cavallaro, *Lubricants: properties and characteristics*, in *Biolubricants*. 2013. p. 24-73.
9. Khalil, M.J.a.H.A., <*Effect of layering pattern on the dynamic mechanical properties and.pdf*>. *Bio Resources*, 2011. **6**: p. 2309-2322.
10. Kalia, S., B.S. Kaith, and I. Kaur, *Pretreatments of natural fibers and their application as reinforcing material in polymer composites-A review*. *Polymer Engineering & Science*, 2009. **49**(7): p. 1253-1272.
11. Sutikno, et al., *Characteristics of natural fiber reinforced composite for brake pads material*. 2018.

12. Stevulova, N., et al., *Properties Characterization of Chemically Modified Hemp Hurds*. Materials (Basel), 2014. **7**(12): p. 8131-8150.
13. Ma, X.T.a.L., *Physical properties and chemical composition of a hemp core*. Journal of Zhejiang Forestry College, 2010. **27**(5): p. 794-798.
14. Ferro, G.A., et al., *Improvements in self-consolidating cementitious composites by using micro carbonized aggregates*. Frattura ed Integrità Strutturale, 2014. **8**(30): p. 75-83.
15. Hatsu Ishida, S.H., Ohio, *United States Patent*. 1996.
16. CarTrade. *Brake Systems in Cars*. 2018 [cited 2019 22 Nov]; Available from: <https://www.cartrade.com/blog/2011/auto-guides/brake-systems-in-cars-17.html>.
17. Hatcher, T. *Vehicle Braking System*. 2014 [cited 2019 23 Nov]; Available from: https://www.motorist.org/aiovg_videos/vehicle-braking-system/.
18. Chan, D. and G.W. Stachowiak, *Review of automotive brake friction materials*. Proceedings of the Institution of Mechanical Engineers, Part D: Journal of Automobile Engineering, 2016. **218**(9): p. 953-966.
19. Ishida H. and D.P. Sanders, *Improved thermal and mechanical properties of polybenzoxazines based on alkyl-substituted aromatic amines*. Journal of Polymer Science Part B: Polymer Physics, 2000. **38**(24): p. 3289-3301.
20. Allen, D.J. and H. Ishida, *Polymerization of linear aliphatic diamine-based benzoxazine resins under inert and oxidative environments*. Polymer, 2007. **48**(23): p. 6763-6772.
21. Sanders, H.I.a.D.P., *Regioselectivity and Network Structure of Difunctional Alkyl-Substituted Aromatic Amine-Based Polybenzoxazines*. Macromolecules, 2000. **33**: p. 8149-8157.
22. Rimdusit, S., et al., *Polybenzoxazine alloys and blends: Some unique properties and applications*. Reactive and Functional Polymers, 2013. **73**(2): p. 369-380.
23. Czichos, H., *Tribology: A system approach to the science and technology of friction, lubrication and wear*. 1978, Amsterdam: Elsevier Science.
24. Tabor, F.P.B.a.D., *The Friction and Lubrication of Solids*. 1964. 424.

25. Gilles, T., *Automotive Chassis :Brakes, Steering and Suspension*. 2005, Thomson Delmar Learning. 551.
26. Dowson, N.C.W.a.D., *Distribution of wear rate data and a statistical approach to sliding wear theory*. *Wear*, 1987. **119**(3): p. 295-312.
27. J. Karger-Kocsis, A.M., Z. Major and N. Bekesi, *Dry friction and sliding wear of EPDM rubbers against steel as a function of carbon black content*. *Wear*, 2008. **264**(3): p. 359-367.
28. G. Gopal, L.R.D., Frank D. Blum, *Load, speed and temperature sensitivities of a carbon-fiber-reinforced phenolic friction material*. *Wear*, 1995. **181-183**: p. 913-921.
29. Andersson, S., *Wear simulation*. Advanced Knowledge Application in Practice, 2010.
30. (TIS97-2557), T.I.S. 2557 [cited 2019 21 May]; Available from: www.ratchakitcha.soc.go.th.
31. SIMSCALE. *Finite Element Analysis*. 2019 [cited 2020 5 March]; Available from: <https://www.simscale.com/docs/content/simwiki/fea/whatisfea.html>.
32. X-Engineer. *Euler integration method for solving differential equations*. 2019 [cited 2020 5 March]; Available from: <https://x-engineer.org/undergraduate-engineering/advanced-mathematics/numerical-methods/euler-integration-method-for-solving-differential-equations/>.
33. Shou Kurihara, H.a.Y.A., Motoki Kuroe, *Binder Resin For Friction Material*. 2012: Akebono Brake Industry Co., Ltd.
34. Lertwassana, W., et al., *High performance aramid pulp/carbon fiber-reinforced polybenzoxazine composites as friction materials*. *Composites Part B: Engineering*, 2019. **177**.
35. Idris, U.D., et al., *Eco-friendly asbestos free brake-pad: Using banana peels*. *Journal of King Saud University - Engineering Sciences*, 2015. **27**(2): p. 185-192.
36. Satapathy, B.K. and J. Bijwe, *Performance of friction materials based on variation in nature of organic fibres*. *Wear*, 2004. **257**(5-6): p. 573-584.
37. I. Chukwujike, O.J.a.G.I., *Studies on the Mechanical Properties of Carbonized/Uncarbonized Cornhub Powder Filled Natural Rubber/Acrylonitrile*

- Butadiene Rubber Bicomposite*. International Journal of Scientific and Research Publications, 2015. **5**(4).
38. Belhocine, A. and W.Z.W. Omar, *Three-dimensional finite element modeling and analysis of the mechanical behavior of dry contact slipping between the disc and the brake pads*. The International Journal of Advanced Manufacturing Technology, 2016. **88**(1-4): p. 1035-1051.
 39. Söderberg, A. and S. Andersson, *Simulation of wear and contact pressure distribution at the pad-to-rotor interface in a disc brake using general purpose finite element analysis software*. Wear, 2009. **267**(12): p. 2243-2251.
 40. Zhang, S., et al., *Simulation Study on Friction and Wear Law of Brake Pad in High-Power Disc Brake*. Mathematical Problems in Engineering, 2019. **2019**: p. 1-15.
 41. Ishida, H. and S. Heights, *Process for preparation of other publications benzoxazine*. 1996, Edison Polymer Innovation Corporation: United State.
 42. Wang, F. and Y. Liu, *Mechanical and tribological properties of ceramic-matrix friction materials with steel fiber and mullite fiber*. Materials & Design, 2014. **57**: p. 449-455.
 43. Makridakis, S., Wheelwright, S., and Hyndman, R.J., *Forecasting: methods and applications*. 1998.
 44. Bashir, M., A. Qayoum, and S.S. Saleem, *Influence of lignocellulosic banana fiber on the thermal stability of brake pad material*. Materials Research Express, 2019. **6**(11).
 45. Motaung, T.E. and L.Z. Linganiso, *Critical review on agrowaste cellulose applications for biopolymers*. International Journal of Plastics Technology, 2018. **22**(2): p. 185-216.
 46. Rimdusit, S., W. Tanthapanichakoon, and C. Jubsilp, *High performance wood composites from highly filled polybenzoxazine*. Journal of Applied Polymer Science, 2006. **99**(3): p. 1240-1253.
 47. R. B. Mathur, P.T., and T. L. Dhami, *Controlling the Hardness and Tribological Behaviour of Non-asbestos Brake Lining Materials for Automobiles*. Carbon Science, 2004. **5**(1): p. 6-11.

48. Wang, Q., et al., *Effect of light-delignification on mechanical, hydrophobic, and thermal properties of high-strength molded fiber materials*. Sci Rep, 2018. **8**(1): p. 955.
49. Vasile, M.B.a.C., *Thermal degradation of lignin – A Review*. Cellulose Chemistry and Technology, 2010. **44**(9): p. 353–363.
50. <http://fr.polymerinsights.com/testing/flammability/loi>, *Limiting Oxygen Index (LOI)*. 2019.
51. Jubsilp, C. and S. Rimdusit, *Polybenzoxazine-Based Self-Lubricating and Friction Materials*, in *Advanced and Emerging Polybenzoxazine Science and Technology*. 2017. p. 945-974.
52. Wu, Y., et al., *Effects of glass-to-rubber transition of thermosetting resin matrix on the friction and wear properties of friction materials*. Tribology International, 2012. **54**: p. 51-57.
53. J., B., *Composites as friction materials: recent developments in non-asbestos fiber reinforced friction materials—a review*. Polymer Composites, 1997. **18**(3): p. 378-396.
54. Amirjan, M., *Microstructure, wear and friction behavior of nanocomposite materials with natural ingredients*. 2019. **131**: p. 184-190.
55. al., K.e., *United States Patent*. 2012.
56. Öztürk, B., F. Arslan, and S. Öztürk, *Effects of Different Kinds of Fibers on Mechanical and Tribological Properties of Brake Friction Materials*. Tribology Transactions, 2013. **56**(4): p. 536-545.
57. Cheng, D.-q., et al., *Friction and wear behavior of carbon fiber reinforced brake materials*. Frontiers of Materials Science in China, 2009. **3**(1): p. 56-60.
58. Öztürk, B. and S. Öztürk, *Effects of Resin Type and Fiber Length on the Mechanical and Tribological Properties of Brake Friction Materials*. Tribology Letters, 2011. **42**(3): p. 339-350.
59. Ma, Y., et al., *Performance assessment of hybrid fibers reinforced friction composites under dry sliding conditions*. Tribology International, 2018. **119**: p. 262-269.

60. Suresh, R., et al., *Numerical Simulation & Experimental study of wear depth and Contact pressure distribution Of Aluminum MMC Pin on Disc Tribometer*. *Materials Today: Proceedings*, 2017. **4**(10): p. 11218-11228.
61. Kim, N.H., et al., *Finite element analysis and experiments of metal/metal wear in oscillatory contacts*. *Wear*, 2005. **258**(11-12): p. 1787-1793.





จุฬาลงกรณ์มหาวิทยาลัย
CHULALONGKORN UNIVERSITY

VITA

NAME Nuttarika Kunaroop

DATE OF BIRTH 15 March 1996

PLACE OF BIRTH Bangkok

INSTITUTIONS ATTENDED Bachelor of Engineering (B.Eng.)

PUBLICATION The 29th Thai Institute of Chemical Engineering and Applied Chemistry Conference (TICChE2020). Bangkok, Thailand 2020. p.75-80
Nuttarika Kunaroop, Phattarin Mora, Sarawut Rimdusit, Chanchira Jubsilp
Effects of Graphite and Carbonized Hemp Hurd Contents on Thermal and Mechanical Properties of Polybenzoxazine Friction Composites